



Effect of Expansion Level and Relief to Shear Layer in a Suddenly Expanded Flow: A CFD Approach

Ridwan¹, Muhammad Ammar Rusydi Rosnin¹, Abdul Aabid², Sher Afghan Khan^{1,*}, Jaffar Syed Mohamed Ali¹, Mohd. Azan Mohammed Sapardi¹

¹ Department of Mechanical and Aerospace Engineering, International Islamic University Malaysia, PO Box 10, Kuala Lumpur 50728, Malaysia

² Department of Engineering Management, College of Engineering, Prince Sultan University, Riyadh, 11586, Saudi Arabia

ARTICLE INFO

Article history:

Received 23 May 2022

Received in revised form 18 October 2022

Accepted 26 October 2022

Available online 15 November 2022

Keywords:

Flow control; supersonic flow; NPR; base pressure; CD nozzle

ABSTRACT

Computational Fluid Dynamics analysis was used to study the effect of expansion level in a suddenly expanded flow for a converging-diverging nozzle expanded to the duct of larger diameter at supersonic Mach number. Parameters include the nozzle pressure ratio (NPR), L/D ratio, and area ratio. The model of the converging-diverging (C-D) nozzle suddenly expanding into the enlarged duct with the cavity was created using the Design Modeler of ANSYS Fluent. The Mach number of the study is 1.6. The area ratio varied from 2.25 to 5.29, and the L/D ranged from 1 to 10. The simulated nozzle pressure ratio (NPR) ranged from 2, 3, 4.25, and 6.375. The outcome demonstrated that the geometric alteration and NPR strongly affect the base pressure. The ambient pressure influences result in lower L/Ds. The cavity of aspect ratio 1 is most effective in raising the base pressure. Increasing the width does not yield any desirable results. However, the location of the cavity played a very significant role in base pressure regulation. The duct's wall pressure and the flow field remained identical with and without control.

1. Introduction

Suddenly expanded flows have applications in many areas, such as the IC engines' rocket nozzle and exhaust ports [1]. The area where relief is available to the flow will form a low-pressure zone whenever sudden expansion occurs. This situation will increase the base drag, contributing as high as 70% of the total drag force. However, the base drag is not of primary concern in subsonic flight Mach number as it contributes at most 10% of skin friction drag [2]. As such, it is vital to study how the sudden flow works so that the base drag, which is detrimental to the flow efficiency, can be reduced using the appropriate control method. Base pressure reduction in suddenly expanded flow is an undesirable effect that requires extensive research. This paper will analyze the base pressure for overexpanded, correctly expanded, and under-expanded flow cases.

* Corresponding author.

E-mail address: sakhan@iium.edu.my

<https://doi.org/10.37934/arfmts.100.3.202229>

This study aims to study the effect of expansion level in a suddenly expanded flow where the flow field of suddenly expanded flow for various expansion level flow at Mach 1.6 will be analyzed. Passive control in the form of cavities will be used. This paper investigates the effect of expansion level in a suddenly expanded flow at Mach number 1.6. The following objectives are highlighted to achieve the aim of this study: To model and simulate the sudden expansion for various expansion levels at supersonic Mach number. To relate the geometry effect on base pressure at supersonic Mach number. To identify the impact of the cavity on base pressure at supersonic Mach number.

2. Literature Review

Suddenly expanded flows offer a broad range of applications, necessitating thorough research. Numerous studies have been done to determine the effectiveness of passive and active control in regulating base pressure. This study aims to assess the effect of various expansion levels in a suddenly expanded flow. The goal of this section is to review the relevant literature. This review highlights some of the most significant results on this subject.

Three differences were identified between the two flows. First, wall shear stresses work only on the wake and the reattached boundary layer in internal flow. Second, through the internal flow of a sudden expansion, the pressure gradients of sections of parallel walls vary. Third, the intersection of jet boundary lines will occur at the Mach lines, the expansion waves originating opposite the internal flow corner. Nonetheless, there is one resemblance between these flows: in both flows, there is a wake region [3]. The study of base pressure development of external flow can be compared with the experimental internal flow as both mechanism is almost the same [4]. Internal flow experiments have several advantages over exterior flow experiments: they use less air, eliminate support devices, and allow for easy measurement of the base pressure in the base region [5,6]. The primary benefit of an internal flow apparatus is that it enables absolute static pressure and surface temperature measurements not only during the expansion's entrance section but also in the wake zone [7,8]. Suddenly expanded flow is characterized by separation, recirculation, and reattachment. The flow is divided by the shear layer into the central flow region and the recirculation flow region [9,10]. Khan *et al.*, [11,12] studied the influence of expansion level on base pressure and reattachment length. Low supersonic Mach number and NPR will exhibit overexpanded flow and high reattachment length. The base region's pressure is reduced since the flow is reattached. Increasing the supersonic Mach number at low NPR caused the nozzle to become highly overexpanded.

Rathakrishnan *et al.*, [13] reviewed the influence of cavities on suddenly expanded flow fields. They concluded that the cavity smoothing impact on the main flow field in the enlarged duct was quite strong for large ducts and that the cavity aspect ratio had a considerable effect on both the flow field and the base pressure. Viswanath and Patil [14] experimented on zero-lift drag characteristics of afterbodies with a square base. They discovered that afterbodies with square bases generate vortical flows ahead of the base, comparable to those on the lee side of a delta wing at incidence. Viswanath [15] investigated the drag reduction of afterbodies by controlled separated flows at high speeds with a standard step height and uniform spacing of steps. He discovered that properly designed multistep afterbodies could significantly reduce total drag (25-50 percent) compared to a blunt base with no modifications. However, compared to traditional axisymmetric afterbodies with circular arcs or conical boattails of an equal base area, the multistep afterbodies have an enormous drag reduction due to the increased momentum losses associated with the separation–reattachment processes at each step.

Azami *et al.*, [16,17] studied the control of suddenly expanded flows with micro-jets, an active control using an experimental method. The experiment proves that micro-jet manages to significantly

base pressure. The adverse effect was nonexistent on the large duct pressure field because the wall pressure distribution is the same with and without control. It is noted that fixing the base pressure level with and without control was affected by NPR. Studied the control of suddenly expanded flows from correctly expanded nozzles. They found that micro-jets can serve as active controllers for base pressure and the micro-jets have no detrimental impact on the wall pressure distribution. They experimented on the expansion level performance for a suddenly expanded flow. They discovered that the Mach number significantly affects the base pressure in the supersonic region [18,19].

Numerous researchers have conducted extensive research on suddenly expanded flow, particularly on base pressure's active and passive control using CFD, experimental approach and optimization method and many more considering other aspects [20-36]. Understanding base pressure behavior and its control mechanism will greatly benefit various aviation and space programs. Controlling base pressure facilitates decreasing base pressure in combustion chambers to enhance mixing and increasing base pressure in rockets and missiles to reduce base drag. Therefore, this paper aims to investigate the control of base pressure with passive control in the form of cavities at various expansion levels.

3. Methodology

3.1 Governing Equations

The fundamental governing equations of fluid dynamics are used for the Computational Fluid Dynamic analysis: the continuity, the momentum, and the energy equation. For incompressible flow, the volume flow rate is even at each cross-section of a stream tube.

$$\dot{Q} = AV \quad (1)$$

where A is the cross-section of the stream tube, and V is the velocity of the fluid. For compressible flow, the mass flow rate is constant at any cross-section of a stream tube.

$$\dot{m} = \rho AV \quad (2)$$

where ρ is the density of fluid at that cross-section. For three-dimensional compressible flow, the continuity equation is

$$\frac{\partial(\rho U_x)}{\partial x} + \frac{\partial(\rho U_y)}{\partial x} + \frac{\partial(\rho U_z)}{\partial x} \rho = 0 \quad (3)$$

$$\frac{\partial \rho}{\partial t} + \frac{\partial(\rho u_i)}{x_i} = 0 \quad (4)$$

The momentum equation,

$$\frac{\partial(\rho u_i)}{\partial t} + \frac{\partial(\rho u_i u_j)}{\partial x_j} = \frac{\partial P}{\partial x_i} + \frac{\partial}{\partial x_i} \tau_{ij} \quad (5)$$

The energy equation,

$$\frac{\partial}{\partial t} \left[\rho \left(e + \frac{v^2}{2} \right) \right] + \frac{\partial}{\partial x_j} \left[\rho u_j \left(e + \frac{v^2}{2} \right) + P + q_j - u_i \tau_{ij} \right] = 0 \quad (6)$$

where, τ_{ij} is viscous stress tensor, q_i is heat flux, ρ is gas density, P is gas pressure, V is velocity modulus, and U is instantaneous velocity.

The calorically perfect gas equation is constructed from specific enthalpy and specific internal energy equations.

$$\frac{c_p}{R} = \frac{\gamma}{\gamma-1} \quad (7)$$

The isentropic process makes the nozzle flow adiabatic and irreversible. The isentropic process is then noted as

$$\frac{p_2}{p_1} = \left(\frac{T_2}{T_1}\right)^{\frac{c_p}{R}} \quad (8)$$

The isentropic relation then is rewritten as

$$\frac{p_2}{p_1} = \left(\frac{T_2}{T_1}\right)^{\frac{\gamma}{\gamma-1}} \quad (9)$$

3.2 Computational Fluid Dynamics

CFD has also become one of the three fundamental methodologies or approaches that may be utilized to solve fluid dynamics and heat transfer problems. The computational aspect refers to studying fluid flow using numerical simulations, which requires computer programs or software packages executed on high-speed digital computers to obtain numerical solutions. The three primary components of a comprehensive CFD analysis are the preprocessor, solver, and postprocessor. CFD has several advantages, including supplementing experimental and analytical methods by providing an alternate, cost-effective method for actual modeling fluid flows [37]. Compared to analytical and experimental fluid dynamics, CFD can provide more detailed, visible, and comprehensive information [38].

The assumptions are created to replicate the flow behavior with the precise physical situation. Choosing the appropriate numerical and mathematical models simplifies the governing equations. In this project, the following assumptions are established to ensure that the numerical simulation methods match the precise physical situation.

- i. The flow is a two-dimensional steady-state flow due to its symmetry along the flow direction.
- ii. The fluid is compressible.
- iii. The velocity flow is turbulent because turbulent viscous dissipation effects are significant.
- iv. The fluid viscosity is a function of temperature.
- v. The pressure at the duct outlet is equal to the ambient air pressure.

3.2.1 Geometry and modelling

The ANSYS software was used in this project utilizing the fluid flow (Fluent) analysis system and Design Modeler used to create geometry for the model. Figure 1 depicts a model of an axisymmetric convergent-divergent nozzle coupled to an axisymmetric duct with annular rectangular cavities. The

model was designed by referring to the experimental setup of Pandey and Rathakrishnan [39]. The duct length varies depending on the L/D ratio, which ranges from 1 to 10.

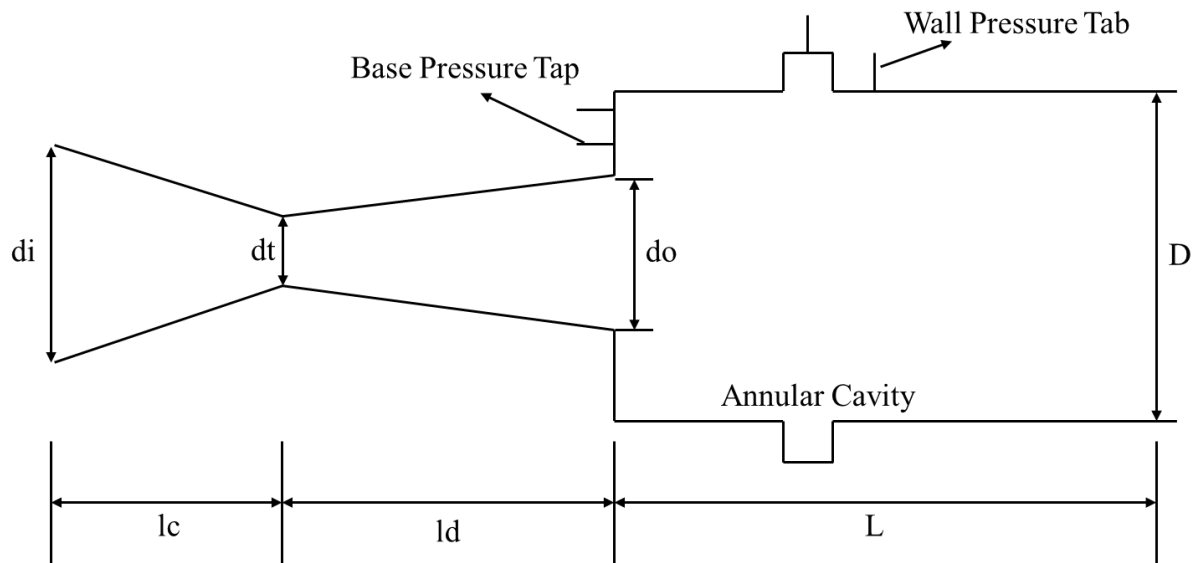


Fig. 1. Convergent-divergent nozzle model with duct and annular cavities

Table 1

The converging-diverging nozzle model geometries

Mach Number, M	1.74
Inlet diameter, d_i	26 mm
Outlet diameter, d_o	10 mm
Convergent length, l_c	17 mm
Cavity width,	3 mm
Cavity depth,	3 mm
Taping distance,	3 mm
Duct diameter, D	17 mm
Duct length, L	It depends on the L/D ratio
Throat diameter, d^*	8.52 mm

Referring to Oosthuizen and Carscallen [40], the ratio of exit area to throat area for Mach number 1.74 is 1.3764.

$$\frac{A_e}{A^*} = 1.3764$$

The relationship between throat area and throat diameter is shown by

$$\frac{A_e}{A^*} = \left(\frac{d_o}{d_t^*}\right)^2 = 1.3764 \quad (10)$$

where, $d^* = 8.52\text{mm}$. The divergent length can be determined using trigonometry. The angle for the divergent part is 4° . The divergent distance then is calculated as follows

$$\tan 4^\circ = \frac{x}{l_d} \quad (l_d = 10.58\text{ mm})$$

3.2.2 Meshing and boundary conditions

The second phase, mesh creation, is one of the most critical tasks in the preprocessing stage once the domain geometry is defined. To solve the flow physics within the defined domain geometry, CFD necessitates the subdivision of the domain into several smaller, non-overlapping subdomains. Consequently, a mesh of cells covering the entire domain geometry is generated. The number of cells in the computational domain's mesh significantly impacts the precision of a CFD solution. Normally increasing the number of cells improves the accuracy of the simulation results. However, it is affected by several other parameters, the kind of mesh, the order of accuracy of a numerical method, and the suitability of the techniques chosen [39].

According to the initial assumption, the time was constant for the overall configuration. Since the geometry of the nozzle is axisymmetric, the 2D space was also set to be axisymmetric. Based on the second assumption, the density-based solver was evaluated for this simulation. The energy equation was selected for the model because the flow is compressible and involves heat transfer. The third assumption is flow is regarded as turbulent velocity. Consequently, the k-epsilon (2 equation) model was chosen. The model of k-epsilon was set to Realizable. Ideal gas was considered fluid for the materials. The viscosity was fixed to Sutherland based on the fourth assumption that the fluid's viscosity is a temperature function. Density, specific heat, and thermal conductivity remained unchanged. As stated in the Table 2 below, the zone was classified depending on its distinct type.

Table 2

The boundary conditions zone name and type

Type	Zone name
Axis	axis
Wall	base pressure
	cavity
	duct
	nozzle
Interior	interior surface body
Pressure inlet	nozzle inlet
Pressure outlet	outlet

The pressure inlet value is equivalent to the total gauge pressure and can be calculated as

$$P_{inlet} = P_{gauge} = P_{atm}(NPR - 1) \quad (11)$$

where, $P_{atm} = 1 \text{ atm} = 101325 \text{ Pa}$.

4. Results

4.1 Mesh Independence Check

The same geometry is used for the mesh independence check using three different element sizes. The mesh independence check was done using varying NPR. The element size and the respective number of nodes and elements are depicted in the table below: The goal of the review for mesh independence is to determine the appropriate element size. Higher NPR requires more iterations and computing time. Choosing a proper element size can reduce computing time without compromising accuracy. The density of structured mesh for each element size listed in Table 3 is as follows.

Table 3
Varying element sizes properties

Element size (mm)	Nodes
1.0	607
0.5	2163
0.3	5754

As observed in Figure 2, the mesh density increases as the element size decrease, and the number of elements is more significant for smaller element sizes. The difference between element sizes with the same NPR and design geometry must be less than 20% to determine the appropriate element size for meshing. Generally, 10k iterations are sufficient for solutions to converge, but 20k iterations are used to ensure solutions converge with high accuracy. Referring to Figure 3, element size 0.3 is the most appropriate to be used for mesh since the percentage difference of the base pressure ratio between element size 0.5 mm and 0.3 mm is lower than 20%. Reducing the element size further to 0.1 mm is unnecessary as it will impose a longer computational time.

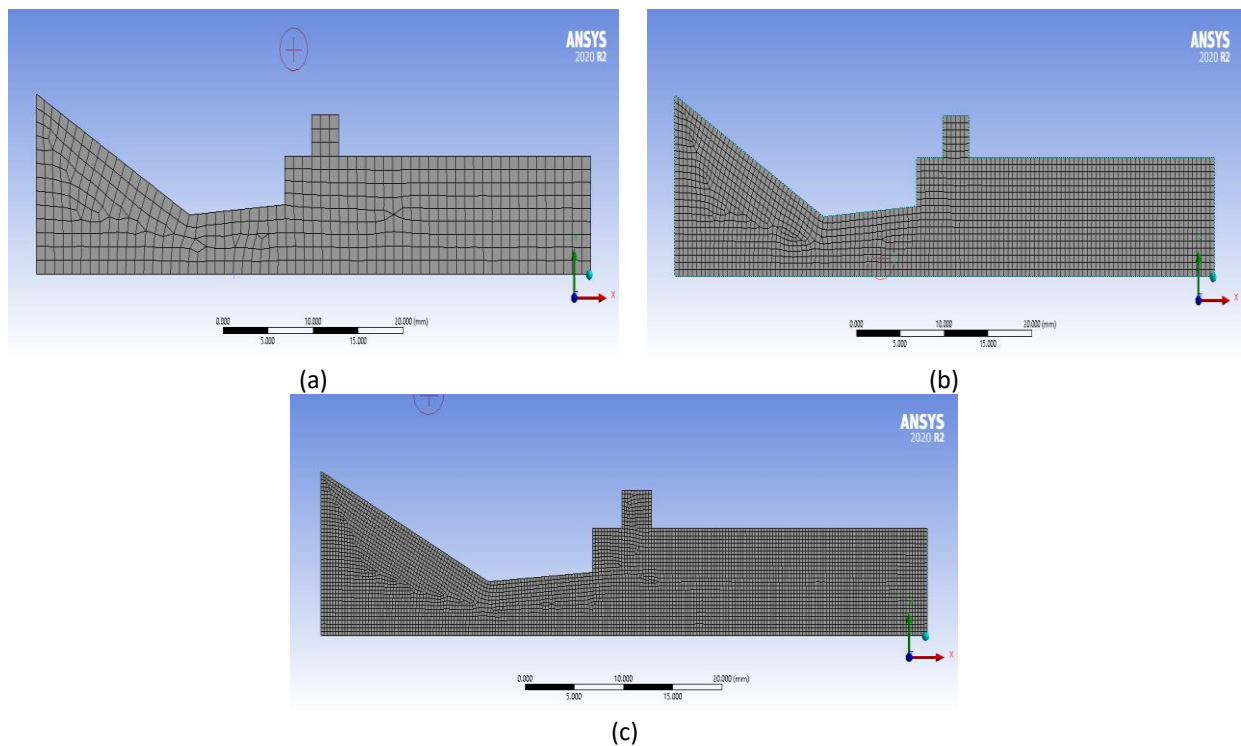


Fig. 2. The structured mesh with an element size of (a) 1.0 mm. (b) 0.5 mm. and (c) 0.3 mm

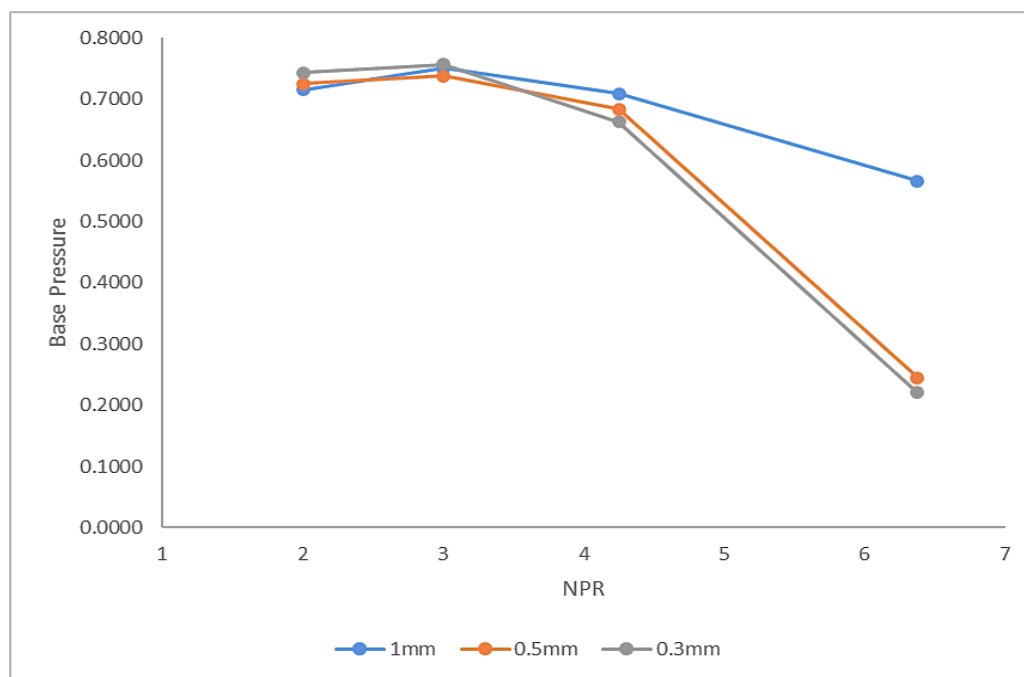


Fig. 3. Base pressure for varying NPR and element size

4.2 Validation of Current CFD Work

The experimental work of Pandey and Rathakrishnan [39] at Mach Number 1.74, NPR of 2.10, 2.65, 2.93, and 3.48, area ratios of 10, 6, and 2.89, and L/D from 1 to 10 was considered as the benchmark results. In this paper, previous work by Pandey and Rathakrishnan [39] with NPR (P_{01}/P_a) 2.65 was chosen to be compared with the present work. Pandey and Rathakrishnan's [39] study shows the base pressure effect at different L/D for the same Mach Number, NPR, and area ratio. For validation, the L/D ratio of this study varied between 2 and 10.

The percentage error was calculated and determined to be less than 10%, putting the current work within the allowable threshold. In addition, Figure 4 illustrates the present and prior work data curves. The curve exhibits a similar trend and small margin error between data points. Therefore, the validation is considered successful. Figure 4 also highlights the effect of varying L/D on base pressure. When the area ratio was 2.89, Pandey and Radhakrishnan [39] noted that the cavity significantly impacts the base pressure. For L/D less than 4, the cavity reduces the base pressure, whereas, for L/D greater than 4, it increases the base pressure. Additionally, Pandey and Radhakrishnan noted that passive control in the form of annular cavities could be utilized to increase the base pressure effectively.

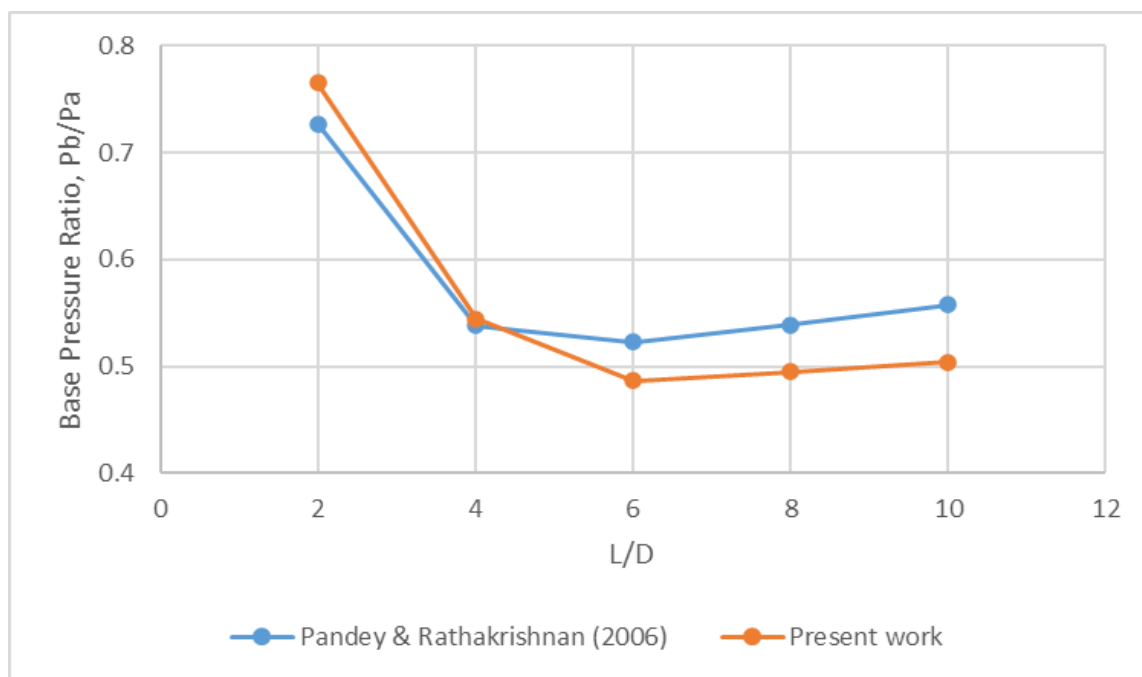


Fig. 4. Present study verification

4.3 Base Pressure Variation with L/D Ratio

Before analyzing the results, it would be better if the physics of the flow field is understood whenever there is a sudden increase in the area of the duct. For supersonic Mach numbers, there is an oblique shock ring, or an expansion fan ring placed at the nozzle exit, dependent on whether the flow is over-expanded or under-expanded, respectively. When there is an expansion, the flow experiences acceleration and turns away. This additional turning, combined with the turning due to free expansion of the flow, will lead to early reattachment and shorter reattachment length. In the case of oblique shock, the shock will turn the flow towards the duct centerline and delay the reattachment, leading to extended reattachment length. Thus, in any case, since the base pressure and flow field oscillations depend on the primary vortex, strength will be significantly influenced by the waves. When annular grooves are in the duct, the flow will experience additional vortex shedding at the cavity. These vortices, being smaller in size, will act as mixing supporters, hence increasing the base pressure.

For an area ratio of 2.25, results are shown in Figure 5(a) to Figure 5(d) at NPRs 2, 3, 4.25, and 6.38 at Mach $M = 1.6$. The level of expansion at these NPRs is 0.47, 0.71, 1.0, and 1.5. When the level of over-expansion is high, the strength of the oblique shock will be high, and with the progressive increase in the NPR, it will decline. The duct size also influences the base pressure values. When the duct size is small, the duct flow field will be influenced by the backpressure; the same is seen in Figure 5. As long as nozzles are under the influence of an adverse pressure gradient, the control is not effective. When the nozzle is operated at perfect expansion, control is marginally effective, resulting in marginal growth in the base pressure; when the nozzle is operating at NPR = 6.38, resulting in under-expanded nozzles. For this NPR value, the control is effective, and there is a significant increase in the base pressure. These results reiterate that control will be at its best whenever nozzles are under-expanded.

Figure 5 until Figure 9 show the base pressure variation with L/D. These figures compare the results for the expanded duct with and without a cavity. The correct expansion of the Mach 1.6 nozzle required the isentropic nozzle pressure ratio (NPR) of 4.25. Consequently, for NPR 2 and 3 of this

study, the flow at the nozzle outlet is overexpanded while under-expanded for NPR 6.375. For the overexpanded scenario, it is apparent that the base pressure decreases sharply for L/D from 1 to 3; the base pressure remains almost constant. That indicates that the effect of the increase in oblique shock strength at the nozzle exit is nullified by the expansion caused by the substantial free space available at the base.

The same trend can be seen for under-expanded cases of area ratios 3.61 and 4.41 in Figure 7(d) and Figure 8(d). Further, the presence of cavity for NPR 6.375 and area ratio of 2.25 and 2.89 seems to be effective in increasing the base pressure as the base pressure is higher than that of the plain duct at all L/D as shown in Figure 5(d) and Figure 6(d). In contrast, the area ratio of 3.61 demonstrates the cavity's minimal effectiveness from L/D 2 to 10, as shown in Figure 7(d). However, the cavity reduces the base pressure in the case of an area ratio of 4.41 for all L/D. For a correctly expanded case at NPR 4.25, the cavity is effective at area ratios 2.25 and 2.89 while marginal for area ratio 5.29 for all L/D as shown in Figure 5(c), Figure 6(c), and Figure 9(c), respectively. The base pressure fluctuates in the area ratio of 4.41, as the cavity is only effective for L/D 4 and 6 while it performs poorly for other L/D. For an area ratio of 3.61, the cavity is effective only at L/D 6.

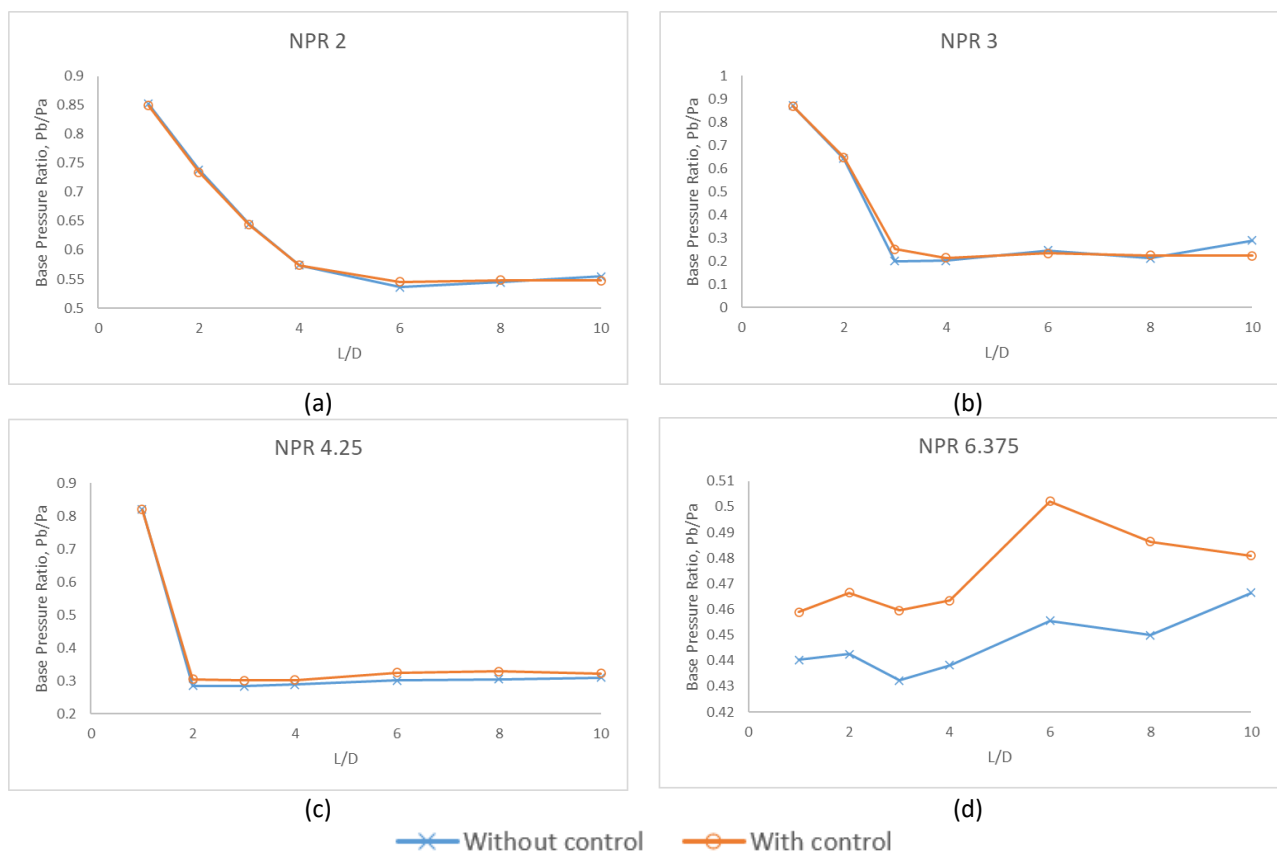


Fig. 5. Base pressure variation with L/D ratio for AR = 2.25

When the duct diameter is raised from 15 mm to 18 mm, the reattachment length will increase due to the increased diameter while keeping all other parameters the same. They exhibit similar patterns in the results barring the case when the nozzle is either ideally expanded or under-expanded. This trend is due to the increased change in the shock pattern and the vortex strength in the separated region.

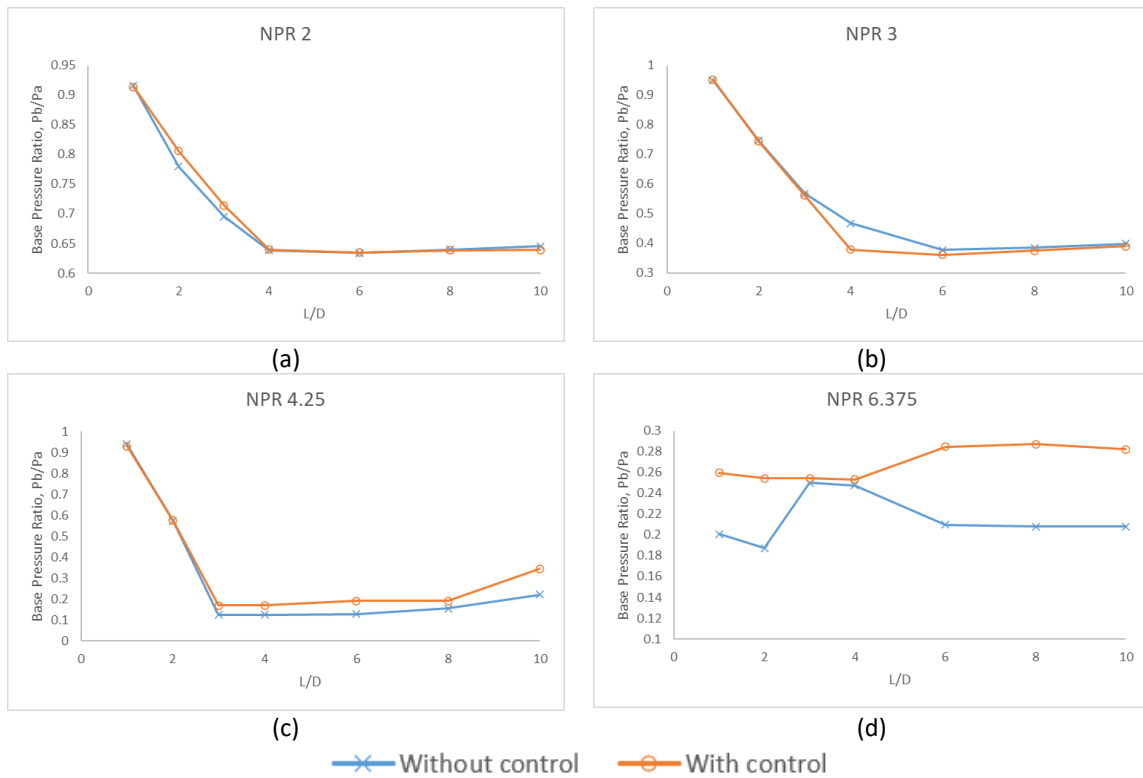


Fig. 6. Base pressure variation with L/D ratio for AR = 2.89

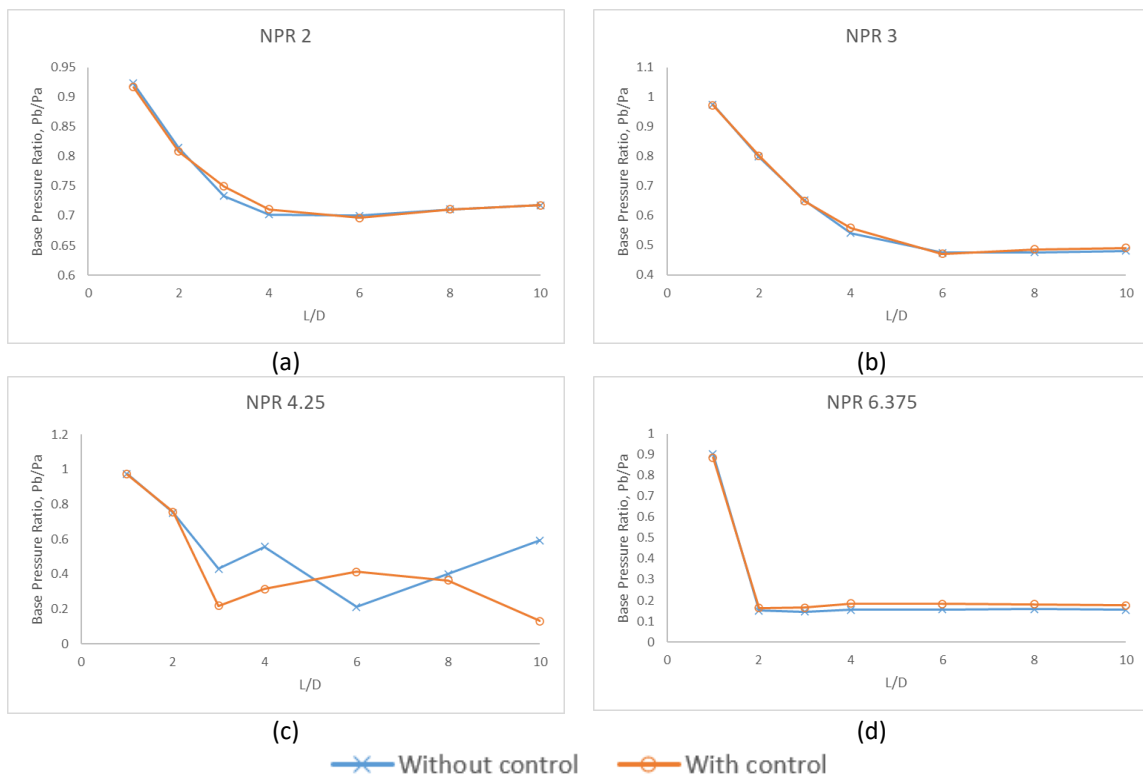


Fig. 7. Base pressure variation with L/D ratio for AR = 3.61

With a further increase in the duct diameter from 17 to 19 mm, the relief available to the flow has increased significantly. This increased area will allow the flow to expand freely and interact with the dividing streamline resulting in the vibratory nature of the flow for correctly expanded nozzles.

Similar results are seen in Figure 8 for a duct diameter of 21 mm. Once again, there are fluctuations in the base pressure values as the acoustic waves are formed when the nozzles are correctly expanded. The results for other NPRs show similar trends as discussed above.

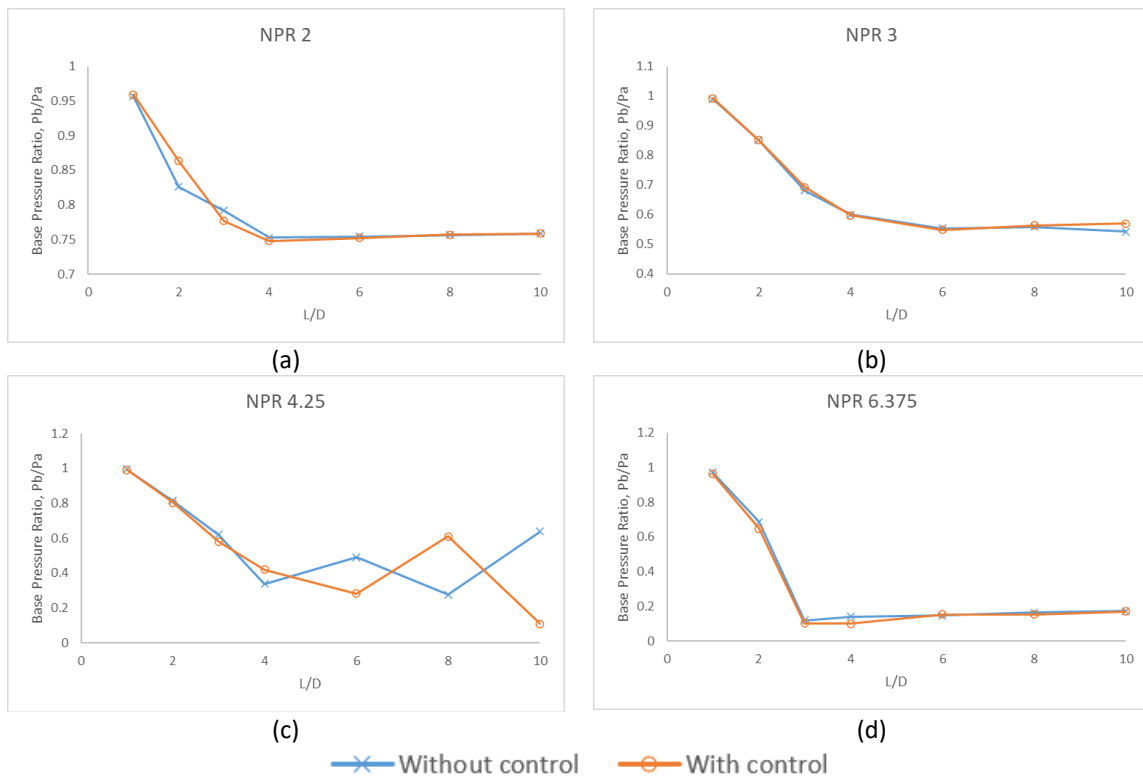
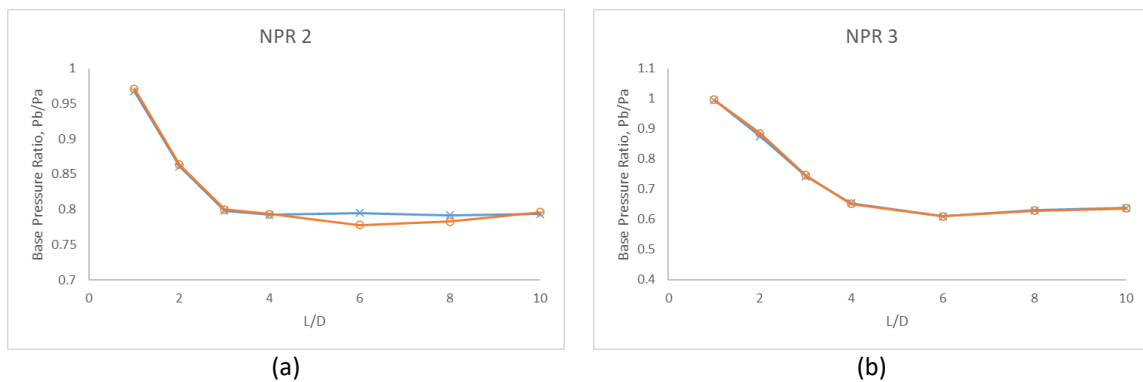


Fig. 8. Base pressure variation with L/D ratio for AR = 4.41

The results for the highest area ratio of 5.89 is shown in Figure 9; they exhibit a similar pattern as discussed above, except the flow has become oscillatory when the nozzle is under-expanded. It may be due to the combined effect of Mach number, area ratio, and level of expansion.



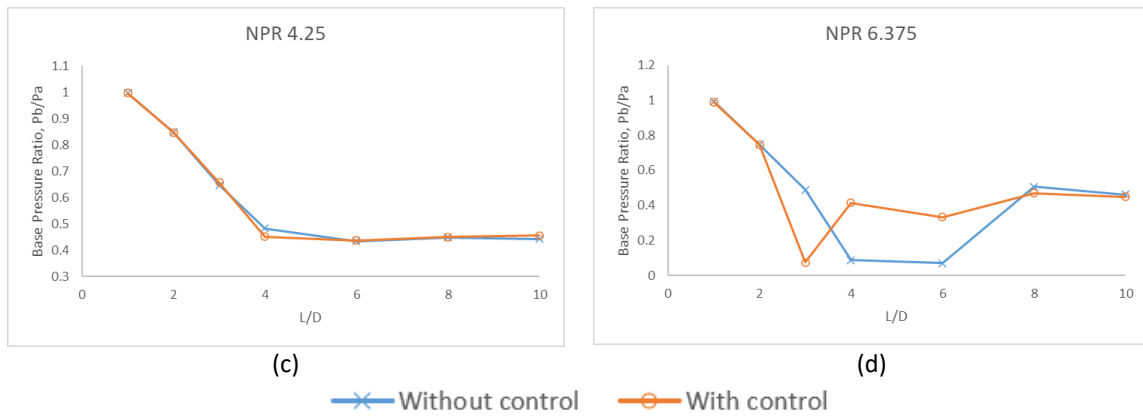
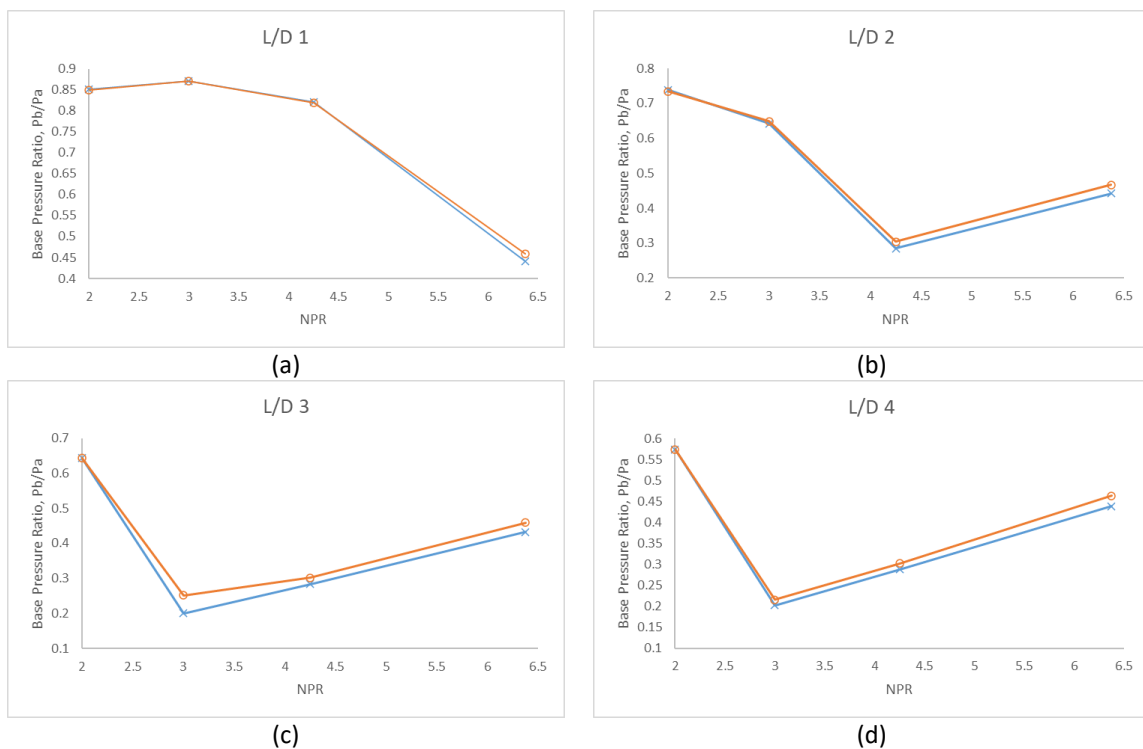


Fig. 9. Base pressure variation with L/D ratio for AR = 5.29

4.4 Base Pressure Variation with Nozzle Pressure Ratio (NPR)

Figure 10 shows the base pressure variation with NPR for an area ratio of 2.25 at various L/Ds. For lower L/D = 1 and 2, the base pressure variation with NPR shows a different pattern. However, the results are as expected for higher duct length L/D = 3 above. Backpressure plays a critical role at lower duct length and dictates the flow field. When cavities are employed, they increase base pressure. Similar results are shown in Figure 11 when duct diameter is marginally improved. As the NPR increases for an area ratio of 2.25 at L/D 1, the base pressure decreases, as shown in Figure 10. The trend continues for L/D 2 until NPR 4.25, after which the base pressure increases. For L/D 3 and above, the base pressure decreases until NPR 3 and rises.



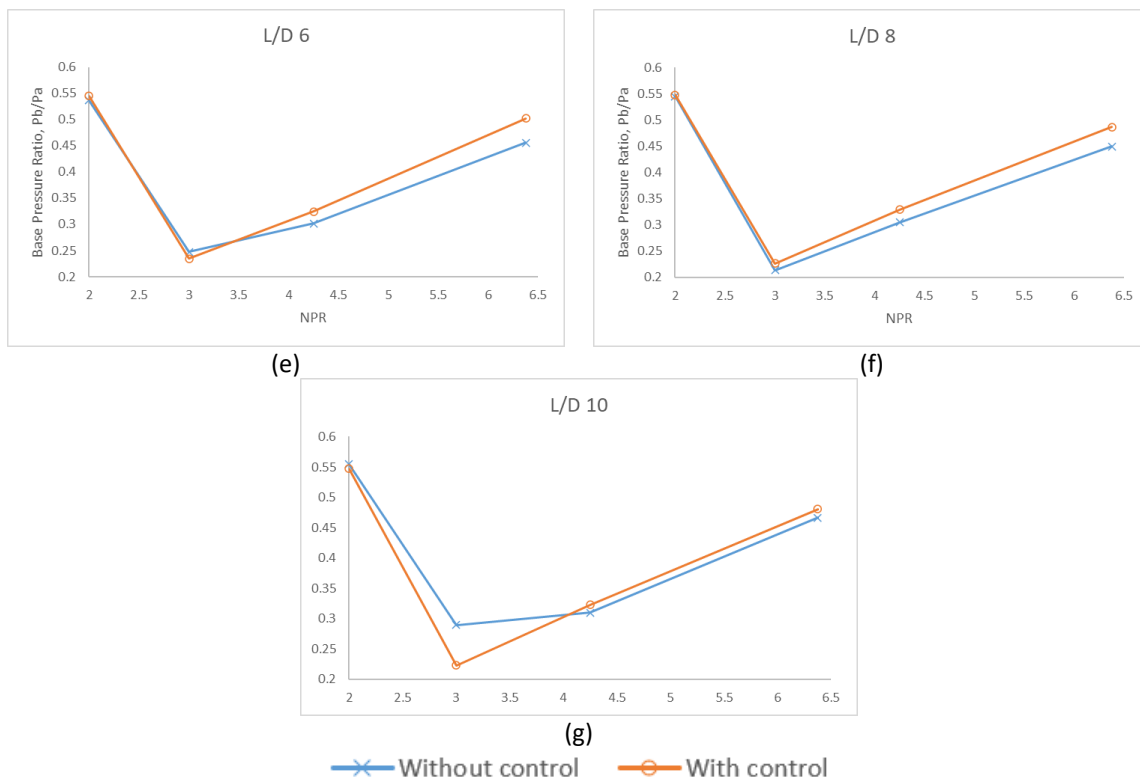
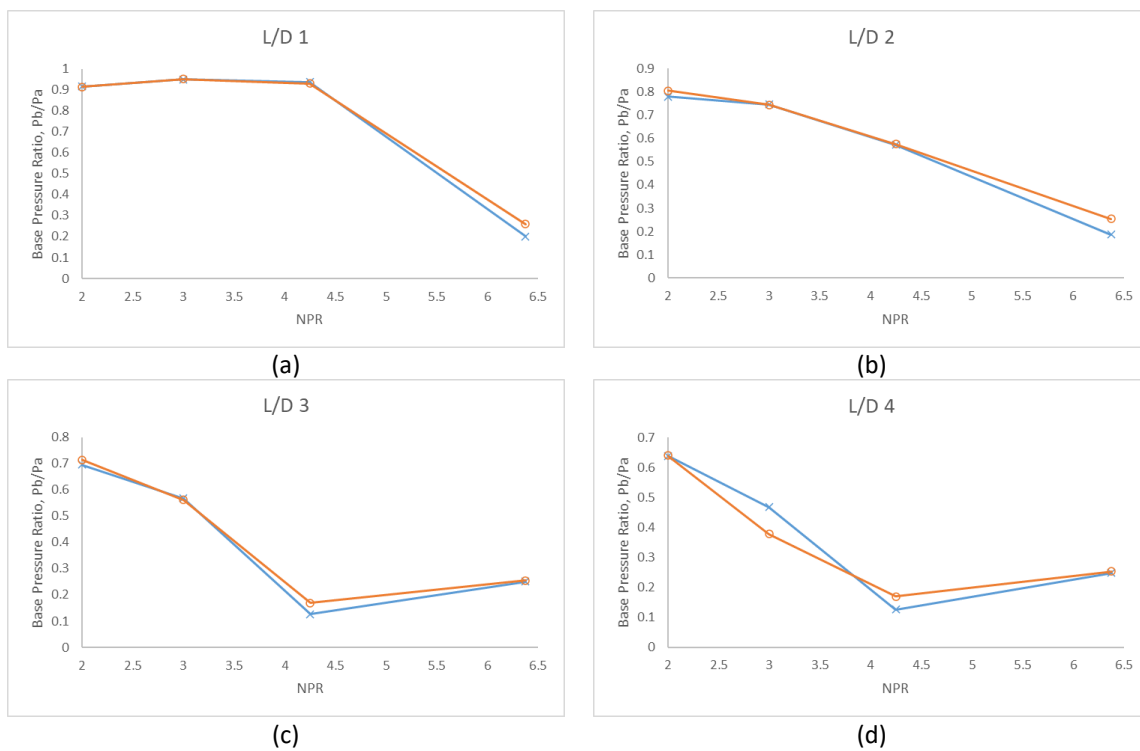


Fig. 10. Base pressure variation with NPR for AR = 2.25

Results for an area ratio of 2.89, as shown in Figure 11. The remainder of L/D follows the same trend, except its base pressure ratio increases after NPR 4.25. The cavity appears to reduce the L/D 8 base pressure at NPR 2, 3, and 4.25. This trend is attributed to the increase in relief available to the shear layer and the influence of ambient pressure.



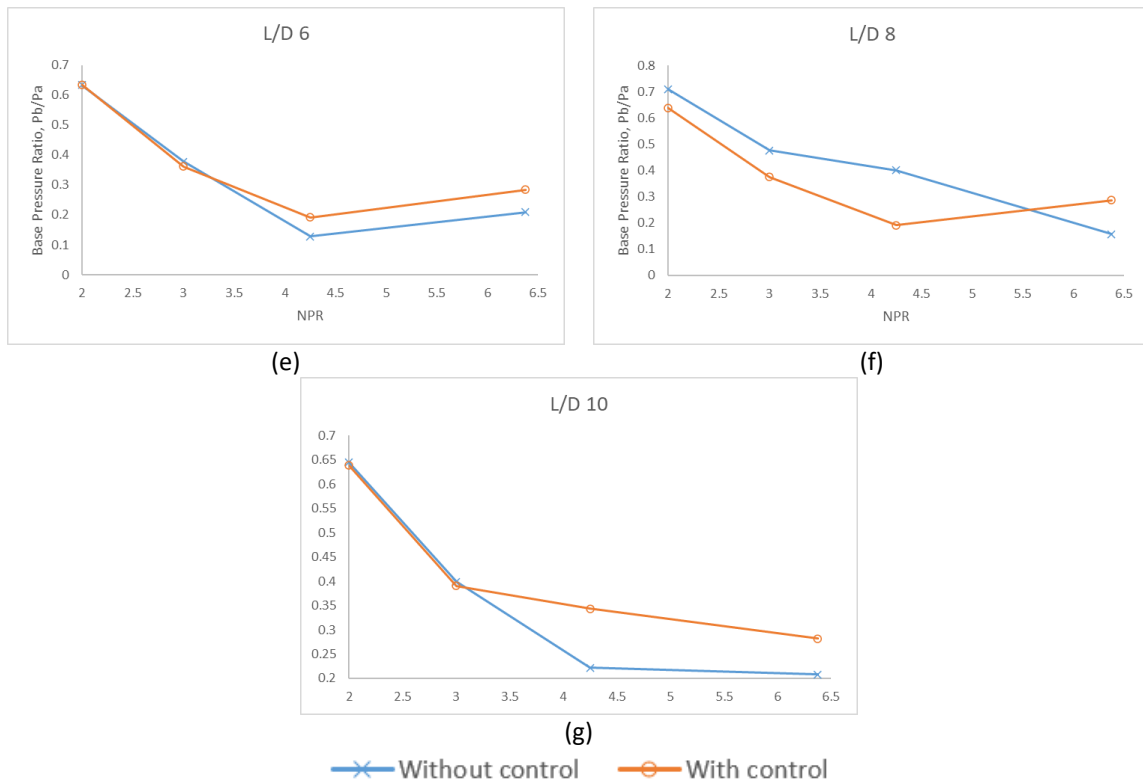
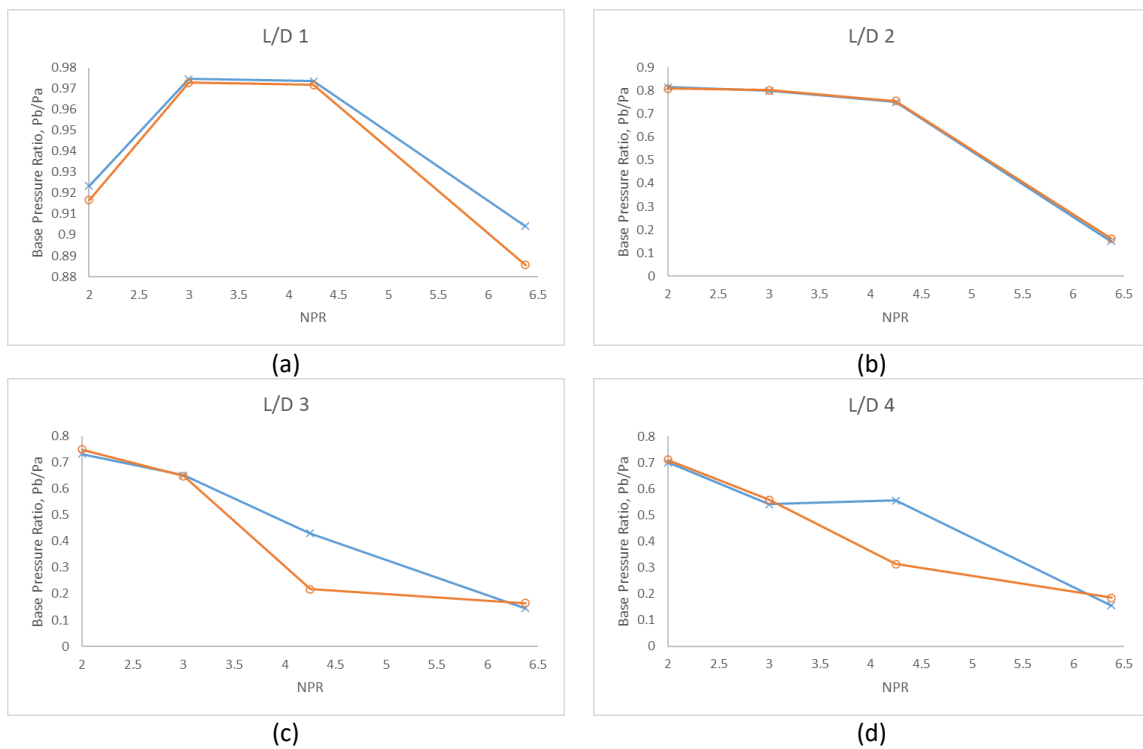


Fig. 11. Base pressure variation with NPR for AR = 2.89

Figure 12 shows results for an area ratio of 3.61. The graph exhibits a declining base pressure trend as long as the nozzles are over-expanded. Control reversal takes place once nozzles are correctly expanded or under-expanded. Also, the cavity at this L/D decreases the base pressure at all NPR. The inefficiency of the cavity is also evident at NPR 4.25 for L/D 3, 4, 8, and 10.



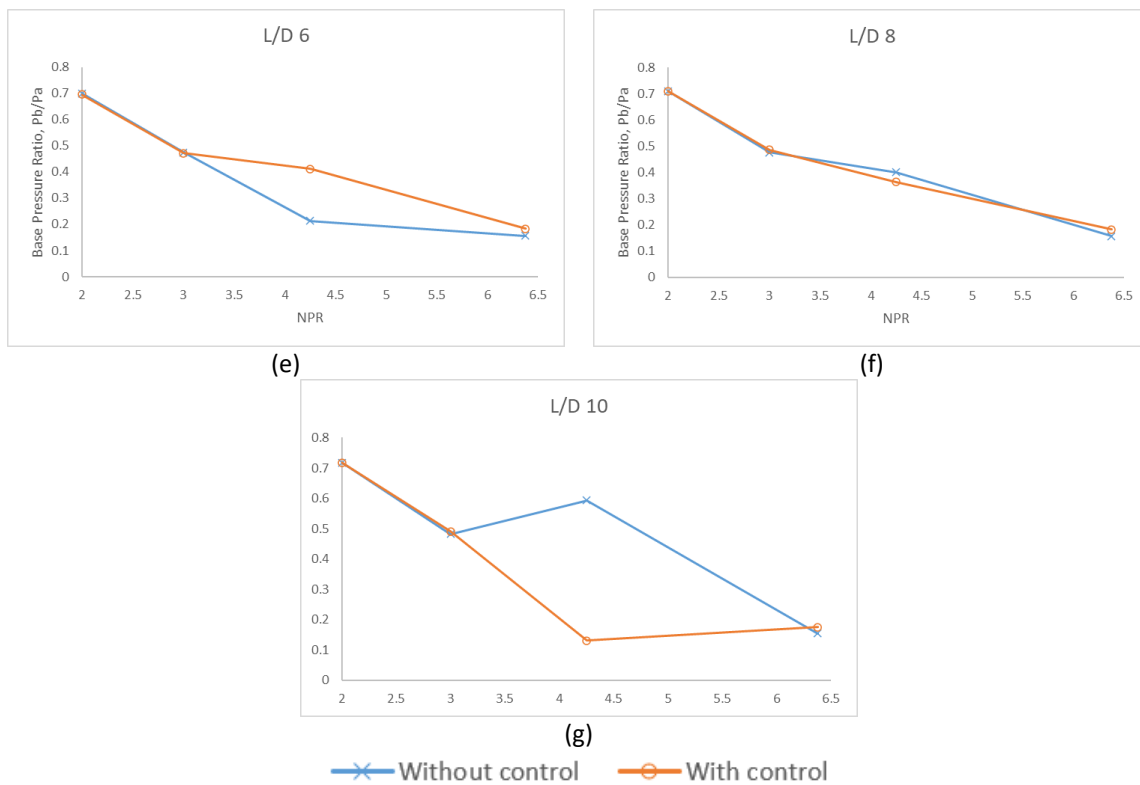
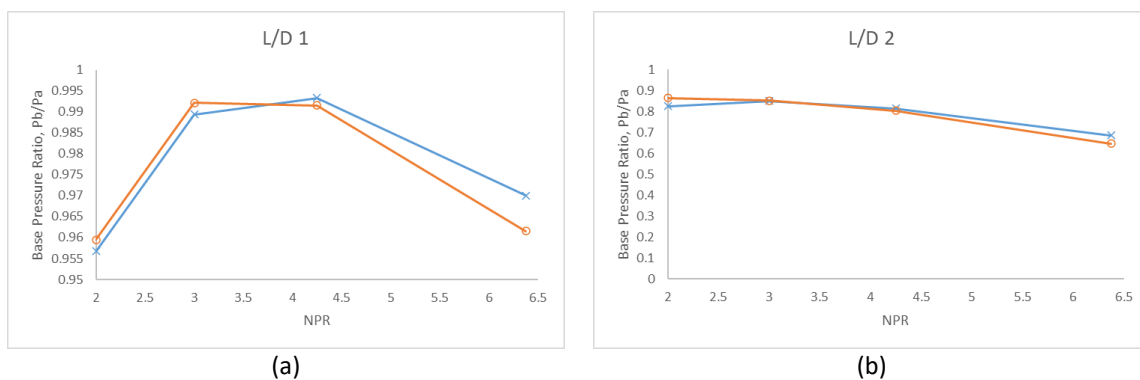


Fig. 12. Base pressure variation with NPR for AR = 3.61

Figure 13 shows a similar pattern to the area ratio of 4.41. For L/D 1, 2, 3, and 10, the cavity reduces the base pressure at NPR 4.25 and 6.375. Figure 14 depicts the result for an area ratio of 5.29, and the cavity also decreases the base pressure at higher NPR. Hence, if one aims to reduce the base pressure, then the results shown in Figure 12 to Figure 14 are the right choice. It is well known that when sudden expansion flow occurs for combustors, the cavities will act as a mixing promoter, resulting in maximum efficiency of the combustion chamber.



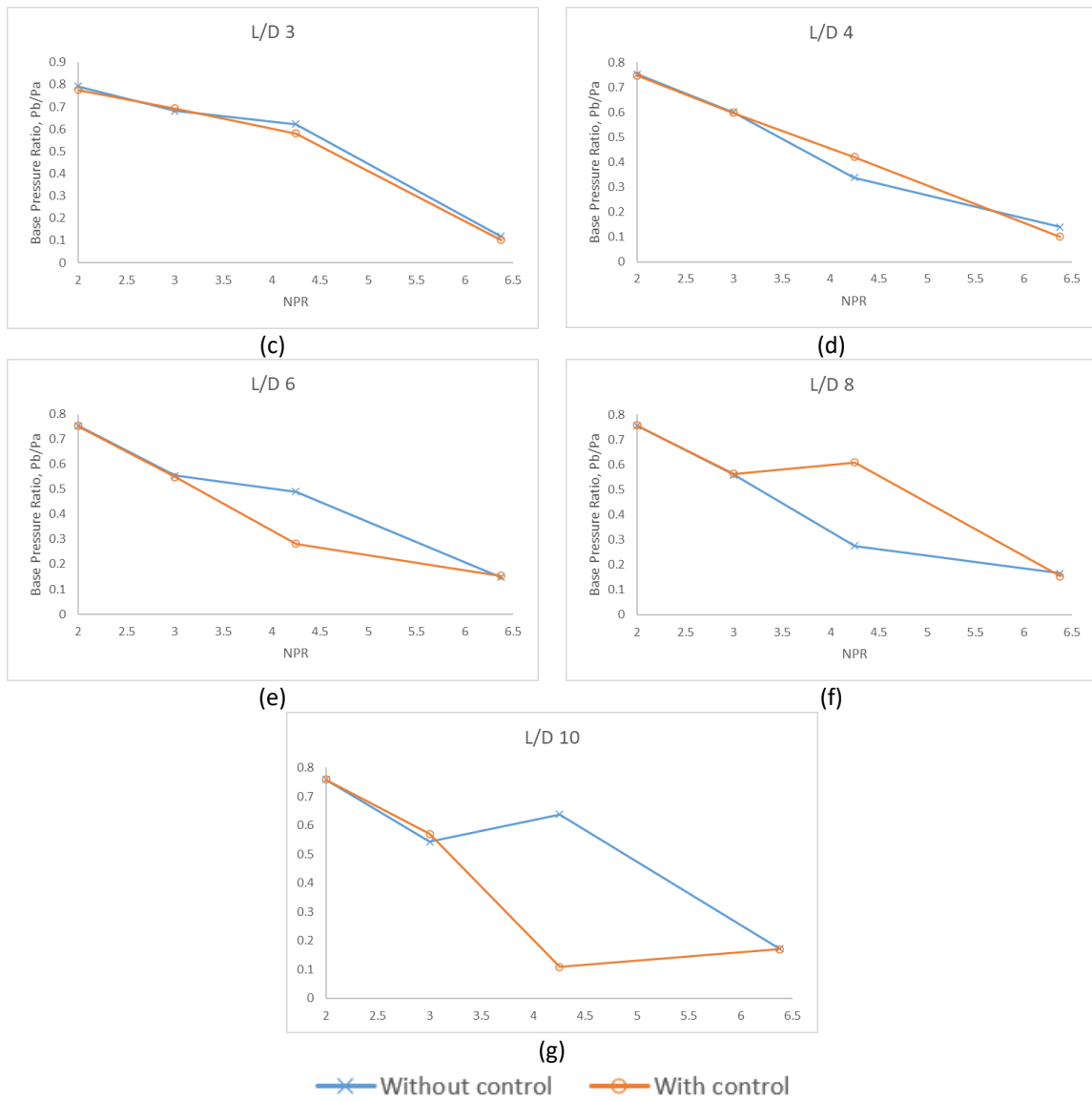
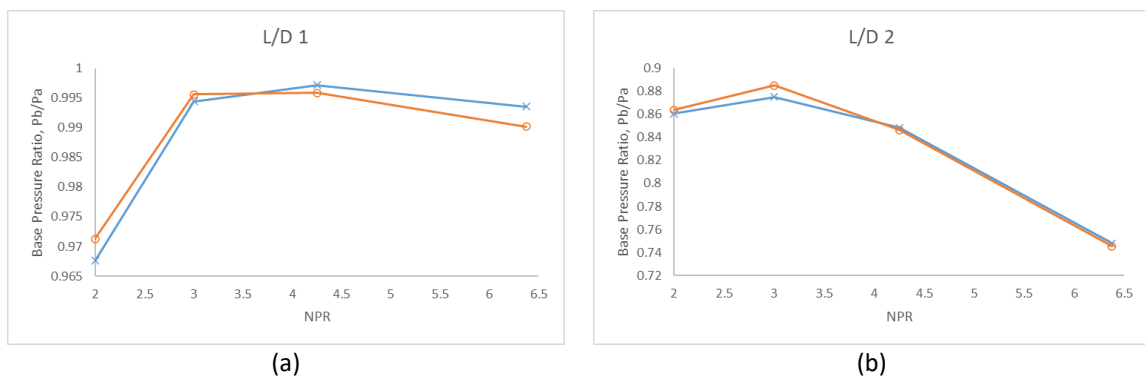


Fig. 13. Base pressure variation with NPR for AR = 4.41



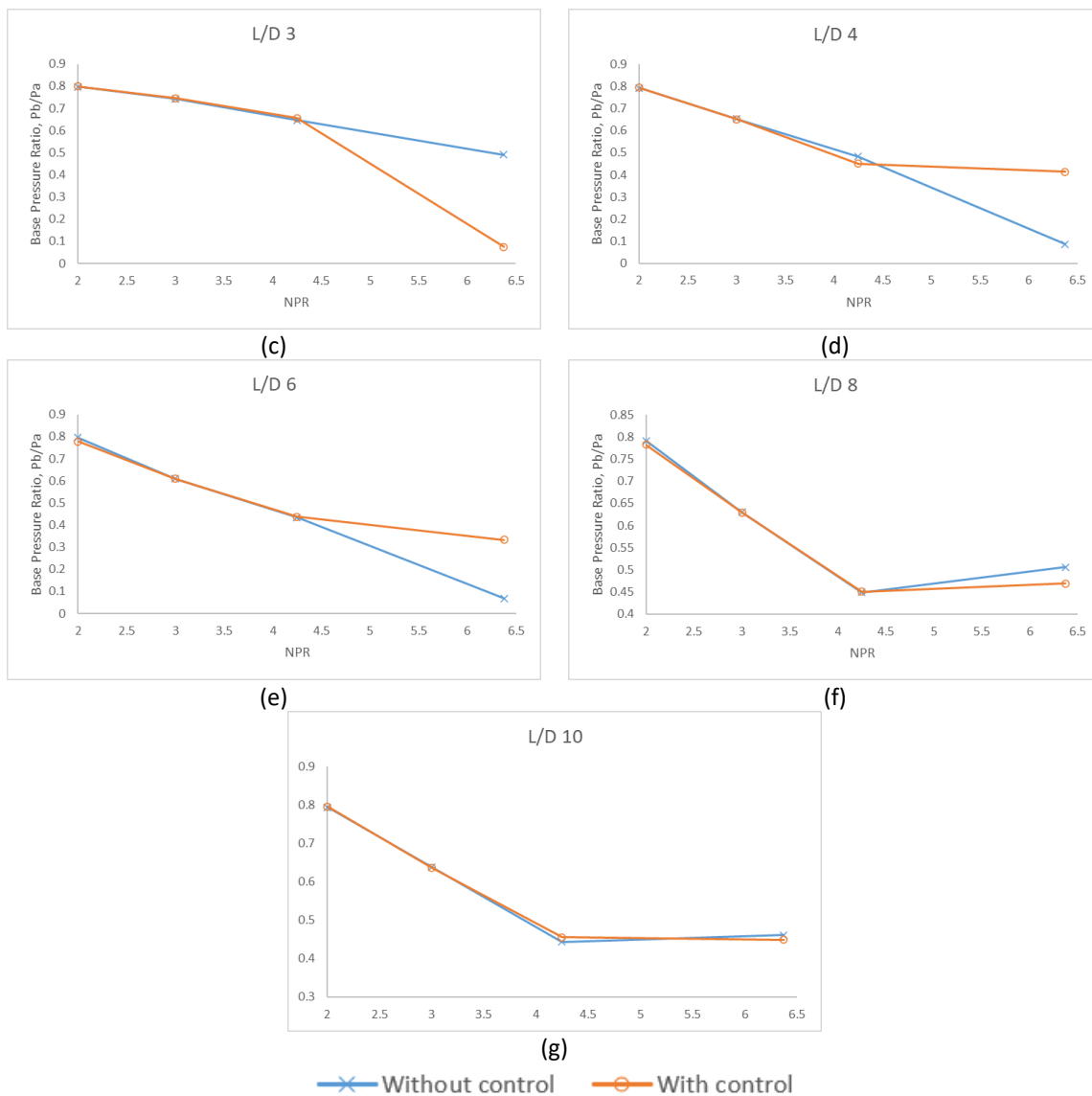


Fig. 14. Base pressure variation with NPR for AR = 5.29

4.5 Base Pressure Variation with Area Ratio

Figure 15 to Figure 18 depict the results of base pressure variation with an area ratio for Mach 1.6 at four pressure ratios of 2, 3, 4.25, and 6.375. The base pressure ratio increases as the area ratio increases for NPR 2, 3, and 4.25. For NPR 2 and 3, the increase in base pressure is steeper as L/D increases. L/D 1 and 2 of NPR 4.25 demonstrate the same pattern; however, L/D 4 and 6 exhibit rapid spikes and decreases in base pressure. For NPR 6.375 of L/D 1 and 2, the initial base pressure decreases as the area ratio increases abruptly at one area ratio and then steadily after that. The base pressure decreases for L/D 4 and 6 as the area ratio increases. However, with an area ratio of 5.29, the base pressure for ducts with cavities increases drastically.

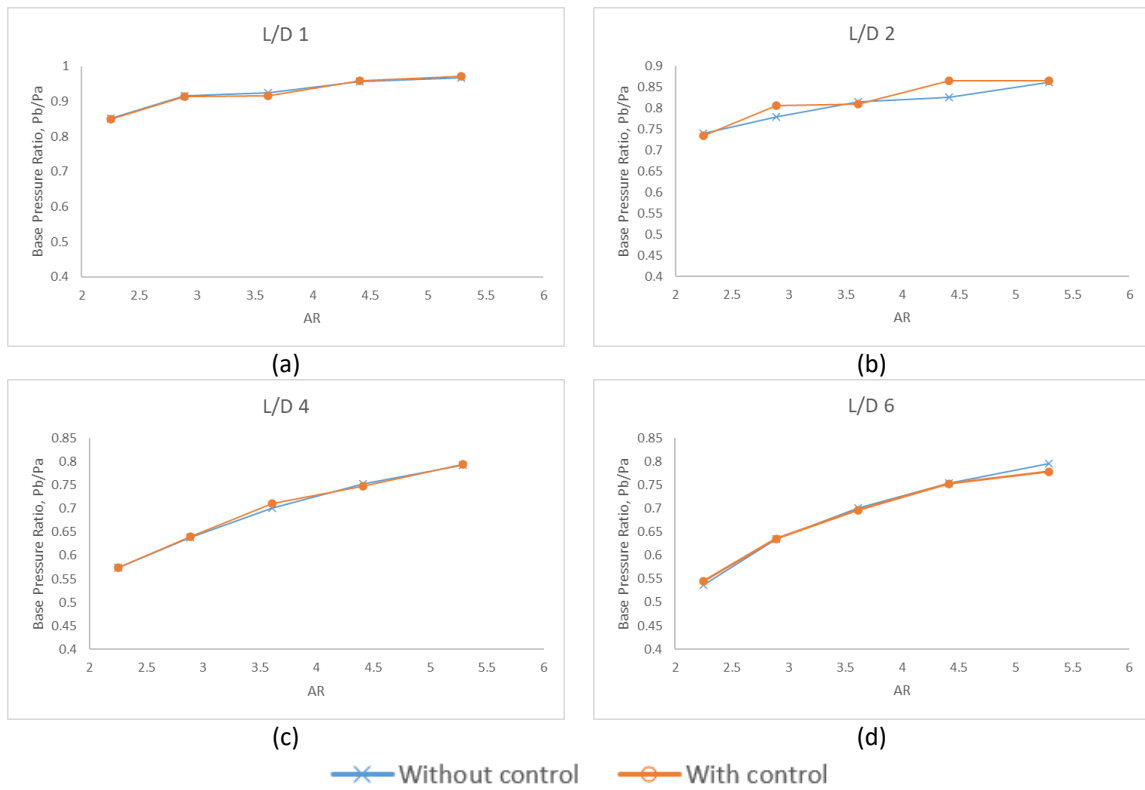


Fig. 15. Base pressure variation with Area ratio for $NPR = 2$

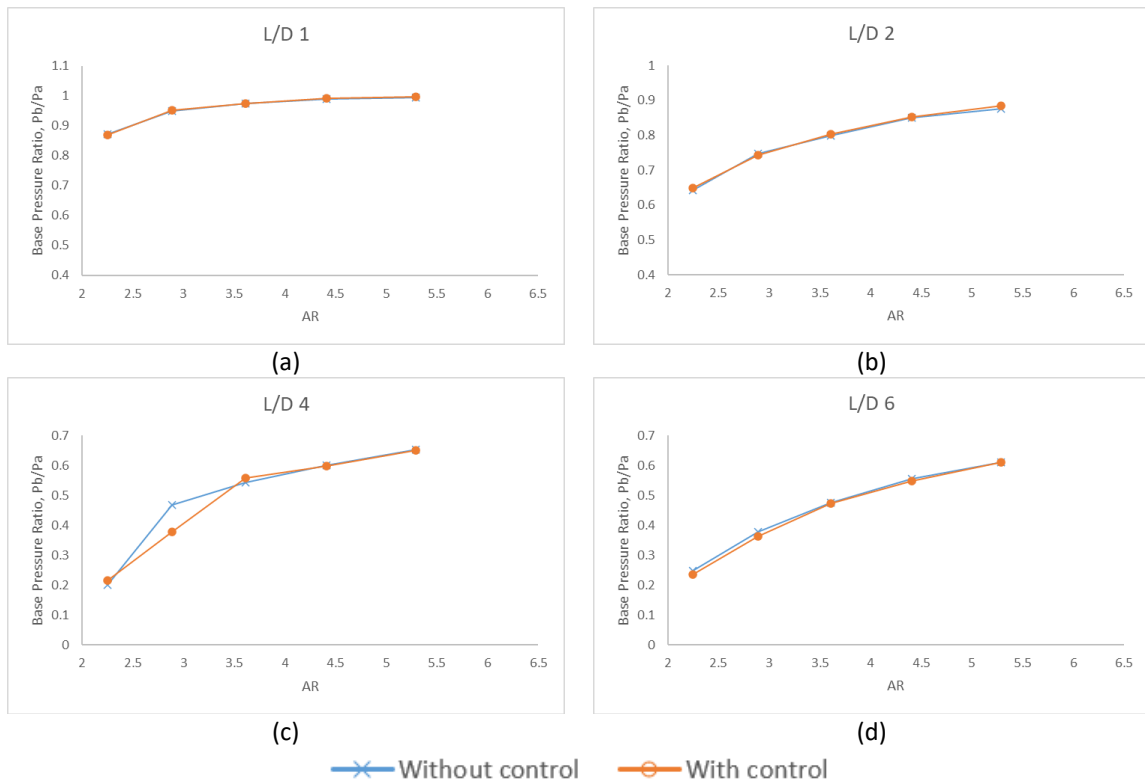


Fig. 16. Base pressure variation with Area ratio for $NPR = 3$

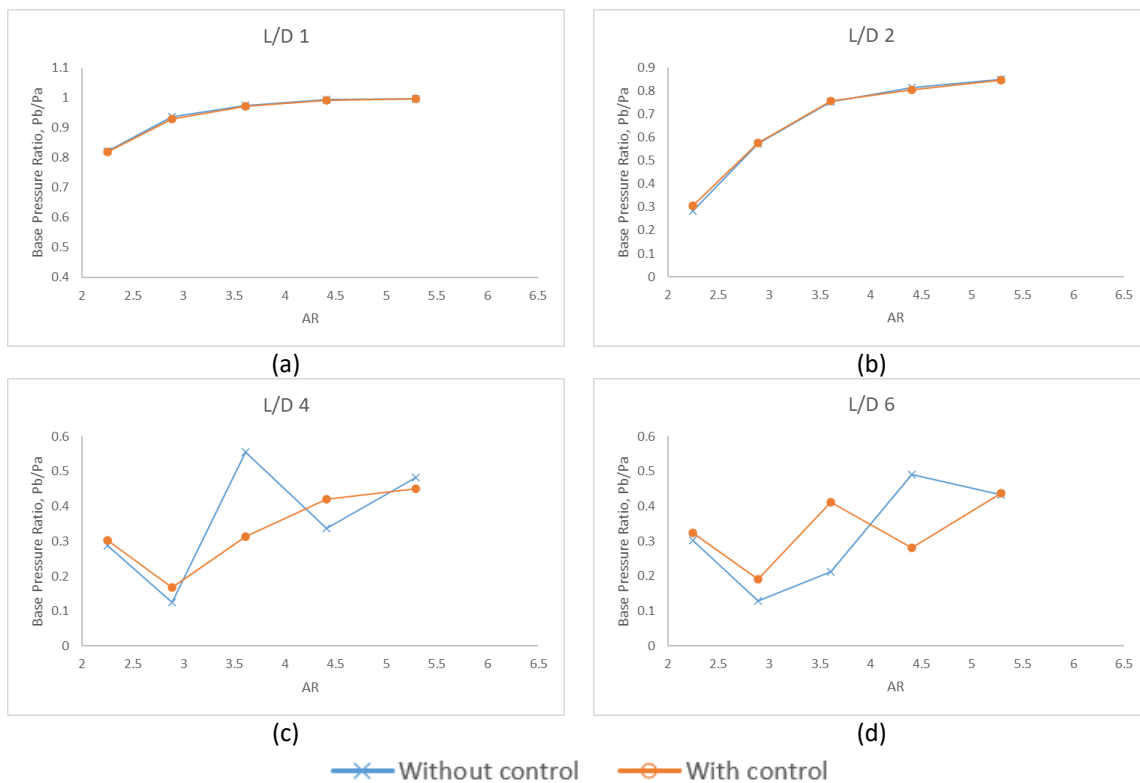


Fig. 17. Base pressure variation with Area ratio for $NPR = 4.25$

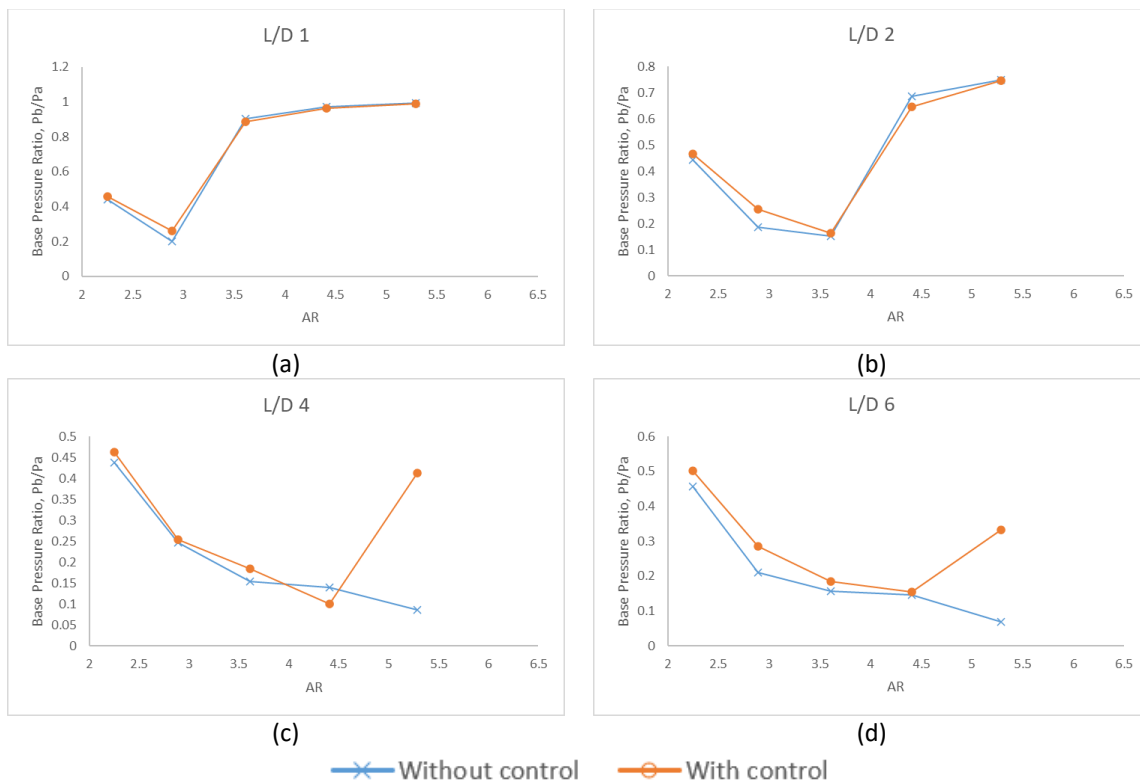


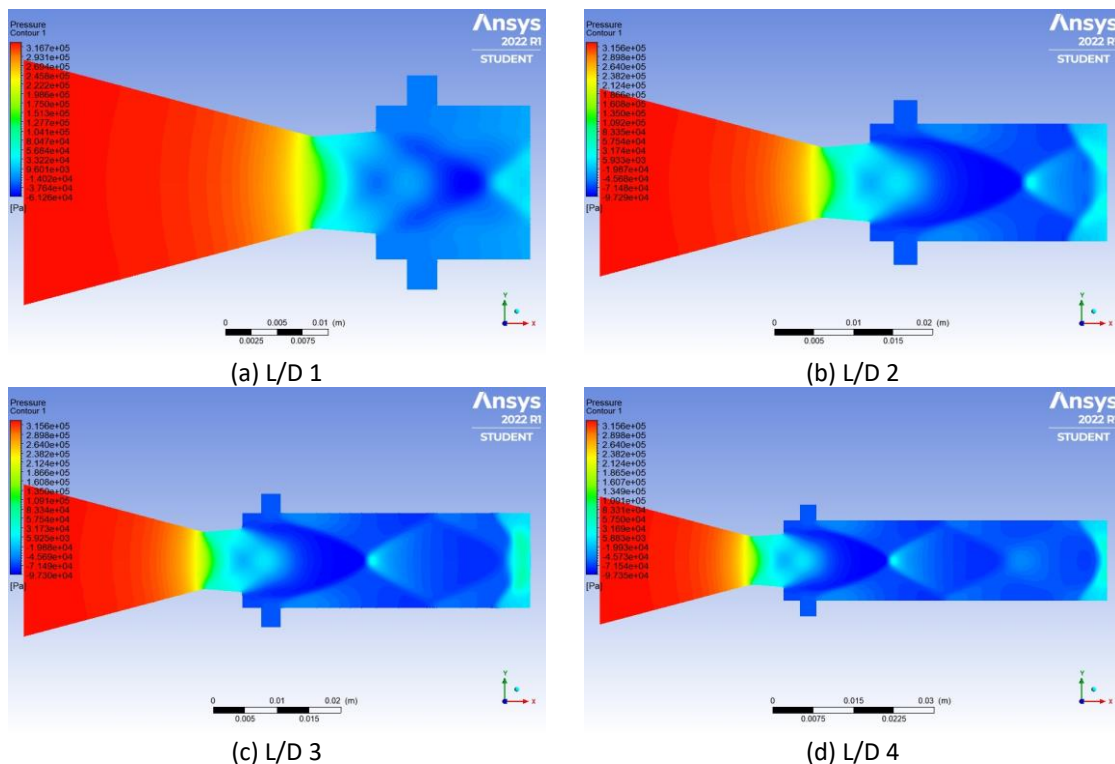
Fig. 18. Base pressure variation with Area ratio for $NPR = 6.375$

4.6 Contour Result: C-D Nozzle Expanded Suddenly into Circular Duct with Control

The contour figures were acquired for Mach 1.6 at various L/D and area ratios with fixed NPR 4. This study demonstrates that a change in geometry affects the base pressure. Additionally, the cavity can raise the base pressure.

The figure below depicts the pressure distribution contours of the converging-diverging nozzle that suddenly expanded to an enlarged duct with the cavity. The red hue denotes the maximum pressure value, while the dark blue color shows the lowest pressure value. When fluid flowing over a body detaches, the reattachment point is the low-pressure zone behind the body that separates the streamlines. Based on all contour data, the hue of the base wall section is nearly constant. Thus, the cavity does not affect the distribution of wall pressure.

Figure 19 to Figure 23 show that the air moves from the region of more significant pressure to the part of lower pressure inside the C-D nozzle, which has suddenly expanded into a duct with a larger cross-sectional area. The air expands abruptly at the base, forming a recirculation region near the base that is low in pressure. It is also much lower than the pressure of the atmosphere in the free stream. The reason is caused by the suction vacuum in the region when the flow exits the nozzle and attaches to the duct. The under-expansion condition at the nozzle output results in the formation of an expansion fan due to the available flow relaxation, while overexpansion and correctly expanded cases at the nozzle exit result in the establishment of oblique shock waves and weak waves at the nozzle exit, respectively.



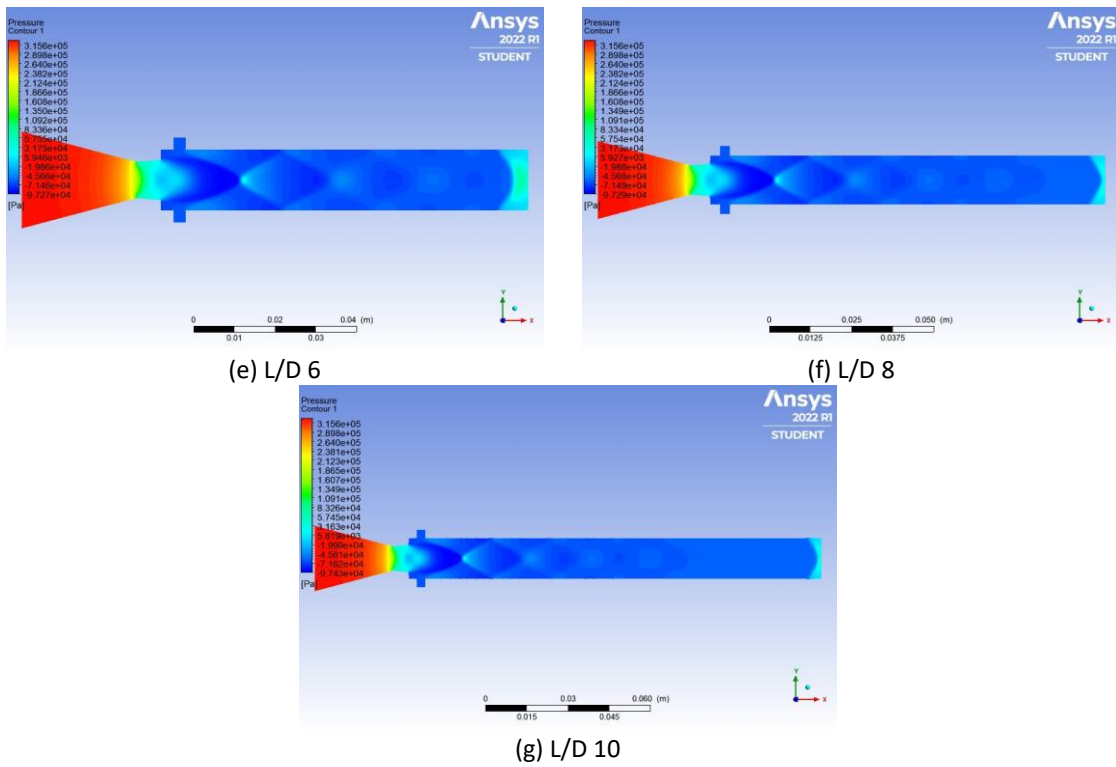
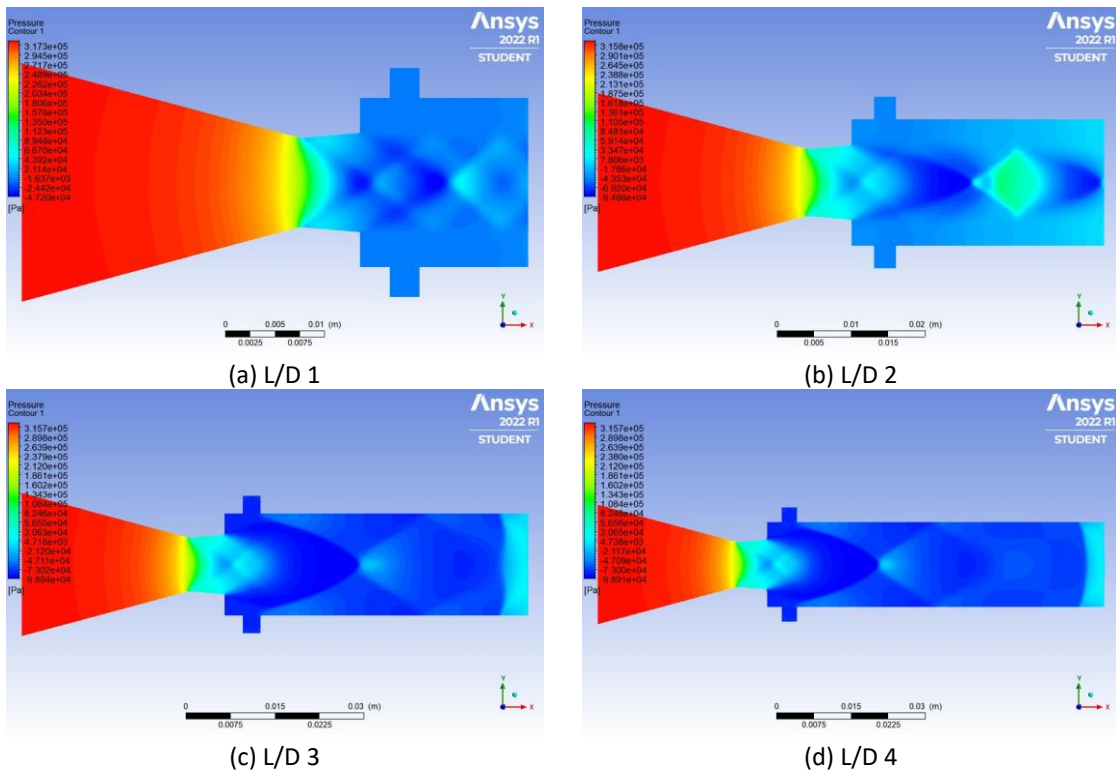


Fig. 19. The contour results for the model with NPR 4, AR 2.25, and ASR 1



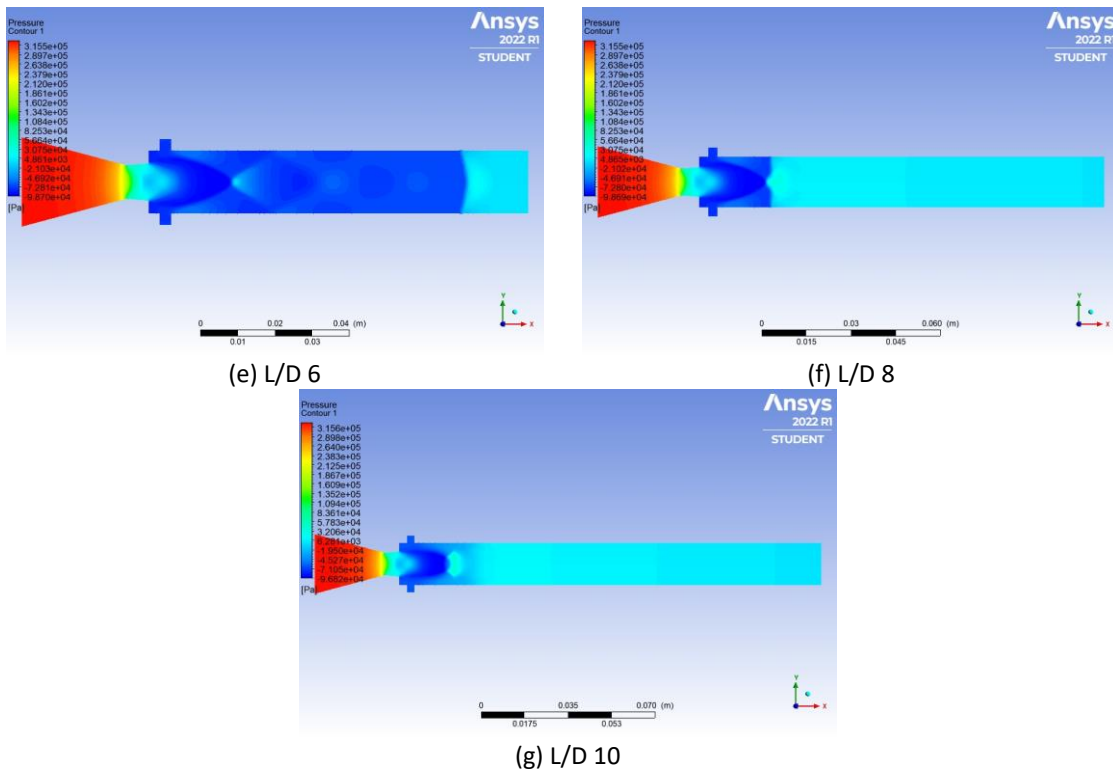
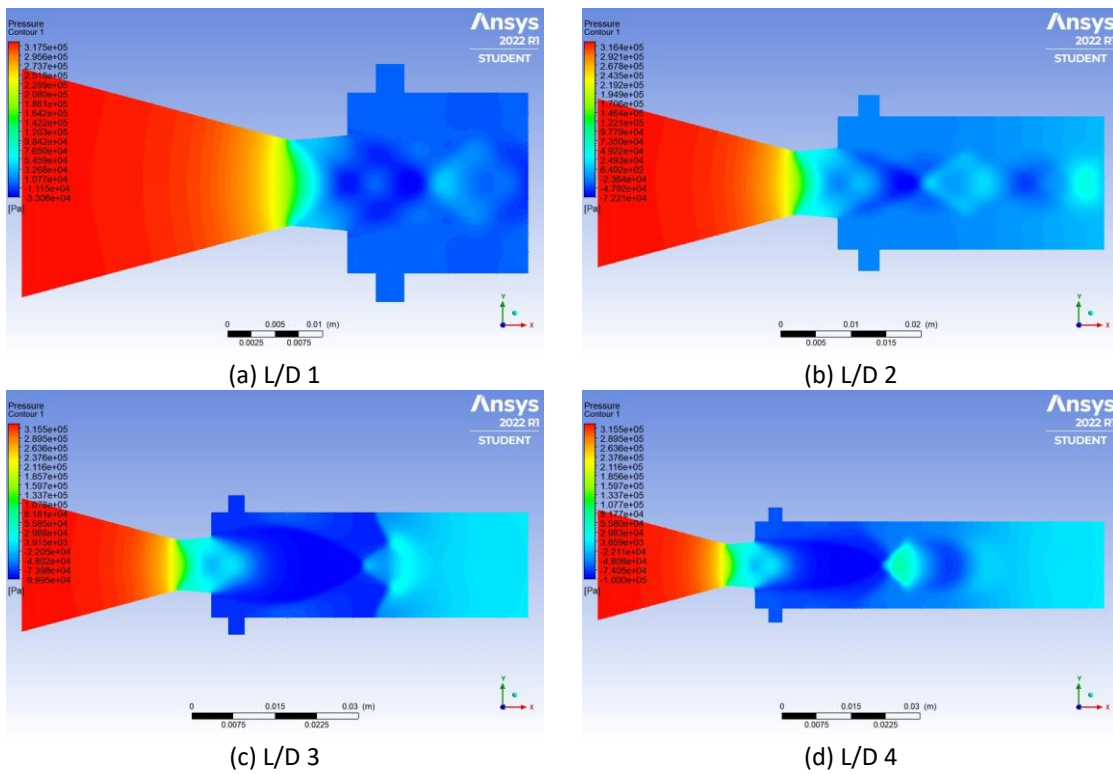


Fig. 20. The contour results for the model with AR 2.89, NPR 4, and ASR 1



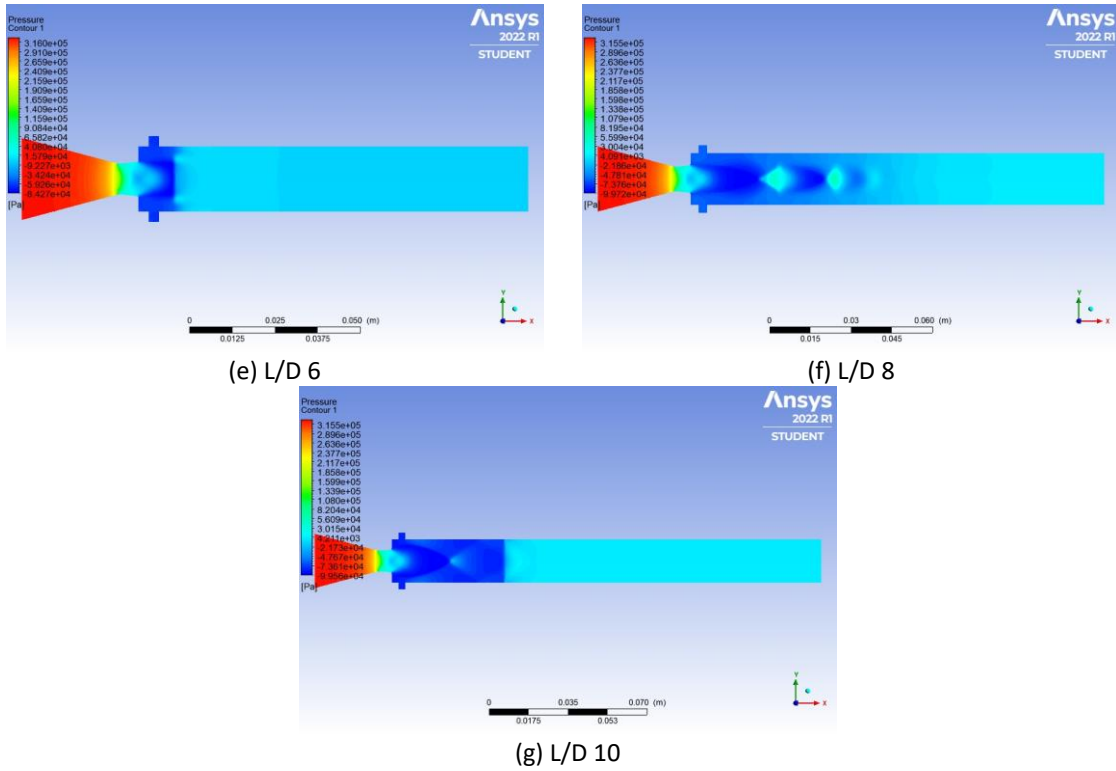
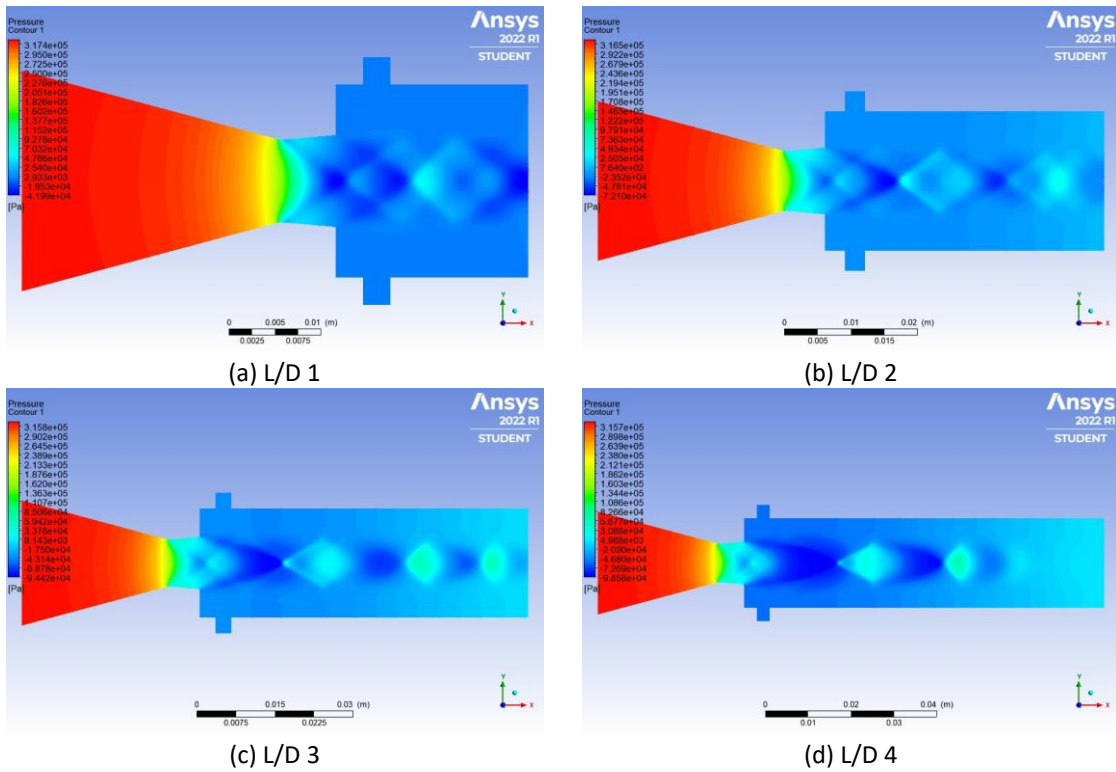


Fig. 21. The contour results for the model with AR 3.61, NPR 4, and ASR 1



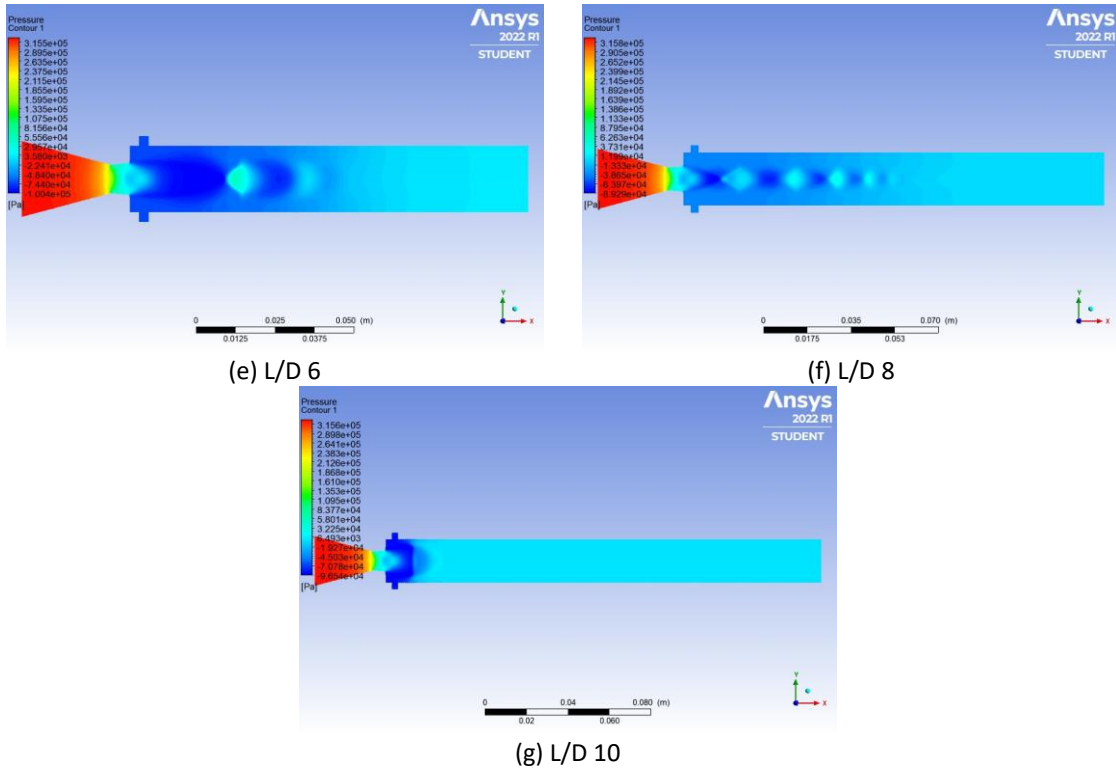
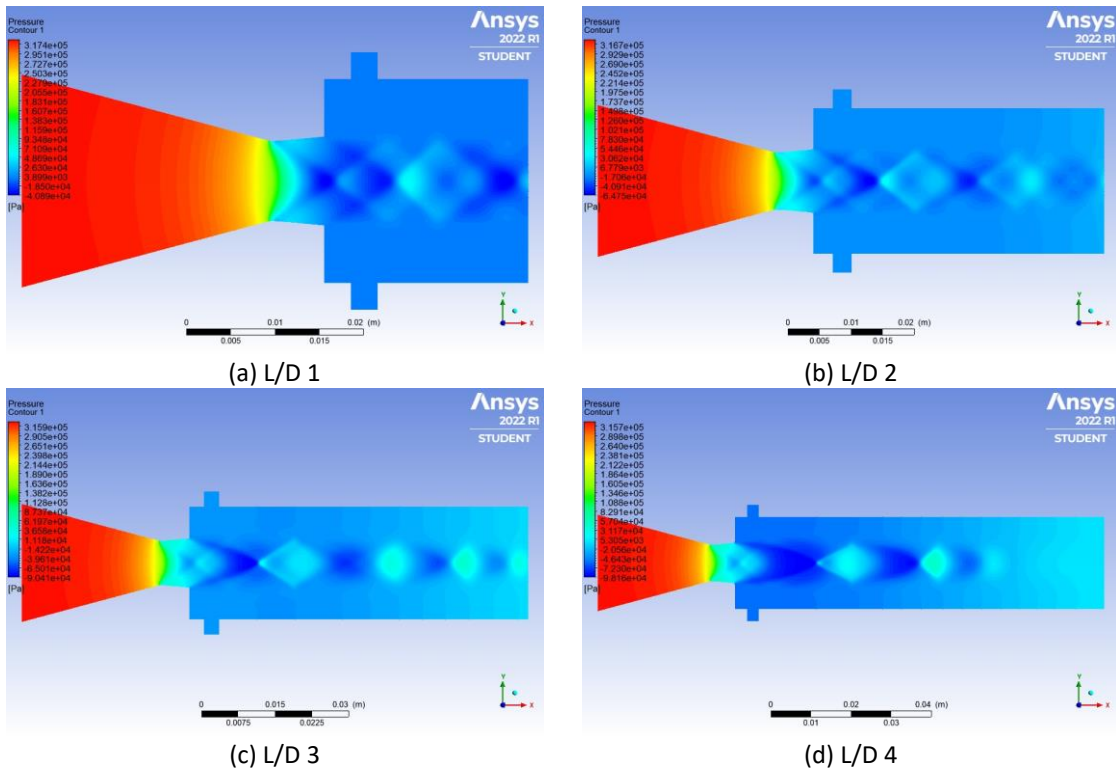


Fig. 22. The contour results for the model with AR 4.41, NPR 4, and ASR 1



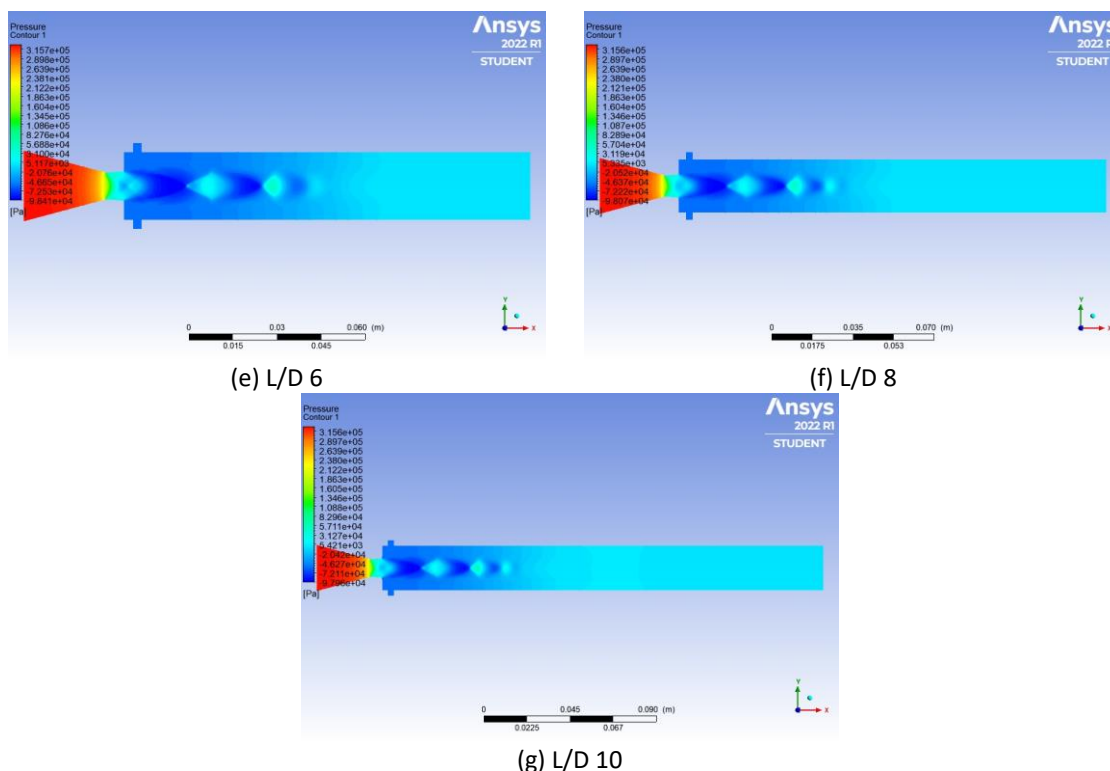


Fig. 23. The contour results for the model with AR 5.29, NPR 4, and ASR 1

5. Conclusions

According to the simulation results of this study, the base pressure is significantly affected by the geometrical parameter to diameter (L/D) ratio, duct area ratio, and nozzle expansion level. When L/D increases, the base pressure ratio decreases due to the decline in the interactions of the back pressure. When nozzles are over-expanded, base pressure attains higher values. However, with the rise in the NPR and reduction in the over-expansion, the base pressure also decreases. In addition, increasing the area ratio increases the base pressure due to the increase in the reattachment length, and the inertia level is kept constant, except for L/D 4 and 6 of NPR 6.375, where increasing the area ratio reduces the base pressure. There are a few recommendations for further research into the passive control of base pressure control. In the future, we can do simulations by varying the aspect ratio of the cavity, cavity's shape, the number of cavities, and the optimum location of the cavity.

References

- [1] Aabid, Abdul, Sher Afghan Khan, and Muneer Baig. "A Critical Review of Supersonic Flow Control for High-Speed Applications." *Applied Sciences* 11, no. 15 (2021): 6899. <https://doi.org/10.3390/app11156899>
- [2] Fharukh, Ahmed G. M., Abdulrehman A. Alrobaian, Abdul Aabid, and Sher Afghan Khan. "Numerical analysis of convergent-divergent nozzle using finite element method." *International Journal of Mechanical and Production Engineering Research and Development* 8, no. 6 (2018): 373-382. <https://doi.org/10.24247/ijimperdddec201842>
- [3] Wick, Robert S. "The effect of boundary layer on sonic flow through an abrupt cross-sectional area change." *Journal of the Aeronautical Sciences* 20, no. 10 (1953): 675-682. <https://doi.org/10.2514/8.2794>
- [4] Hoerner, Sighard F. "Base drag and thick trailing edges." *Journal of the Aeronautical Sciences* 17, no. 10 (1950): 622-628. <https://doi.org/10.2514/8.1750>
- [5] Aabid, Abdul, Ahmed GM Fharukh, and Sher Afghan Khan. "Experimental Investigation of Wall Pressure Distribution in a Suddenly Expanded Duct from a Convergent-Divergent Nozzle." In *2019 IEEE 6th International Conference on Engineering Technologies and Applied Sciences (ICETAS)*, pp. 1-6. IEEE, 2019. <https://doi.org/10.1109/ICETAS48360.2019.9117428>
- [6] Khan, Sher Afghan, Abdul Aabid, and Zakir Ilahi Chaudhary. "Influence of control mechanism on the flow field of

- duct at mach 1.2 for area ratio 2.56." *International Journal of Innovative Technology and Exploring Engineering* 8, no. 6S4 (2019): 1135-1138. <https://doi.org/10.35940/ijitee.F1236.0486S419>
- [7] Akhtar, Mohammad Nishat, Elmi Abu Bakar, Abdul Aabid, and Sher Afghan Khan. "Effects of micro jets on the flow field of the duct with sudden expansion." *International Journal of Innovative Technology and Exploring Engineering (IJITEE)* 8, no. 9S2 (2019): 636-640. <https://doi.org/10.35940/ijitee.I1129.0789S219>
- [8] Akhtar, Mohammad Nishat, Elmi Abu Bakar, Abdul Aabid, and Sher Afghan Khan. "Control of CD nozzle flow using microjets at mach 2.1." *International Journal of Innovative Technology and Exploring Engineering (IJITEE)* 8, no. 9S2 (2019): 631-635. <https://doi.org/10.35940/ijitee.I1128.0789S219>
- [9] Khan, Sher Afghan, Zaheer Ahmed, Abdul Aabid, and Imran Mokashi. "Experimental research on flow development and control effectiveness in the duct at high speed." *International Journal of Recent Technology and Engineering (IJRTE)* 8, no. 2S8 (2019): 1763-1768. <https://doi.org/10.35940/ijrte.B1149.0882S819>
- [10] Faheem, Mohammed, Mohammed Kareemullah, Abdul Aabid, Imran Mokashi, and Sher Afghan Khan. "Experiment on of nozzle flow with sudden expansion at mach 1.1." *International Journal of Recent Technology and Engineering* 8, no. 2S8 (2019): 1769-1775. <https://doi.org/10.35940/ijrte.B1150.0882S819>
- [11] Khan, Sher Afghan, Abdul Aabid, Imran Mokashi, and Zaheer Ahmed. "Effect of micro jet control on the flow filed of the duct at mach 1. 5." *International Journal of Recent Technology and Engineering (IJRTE)* 8, no. 2S8 (2019): 1758-1762. <https://doi.org/10.35940/ijrte.B1148.0882S819>
- [12] Khan, Sher Afghan, Imran Mokashi, Abdul Aabid, and Mohammed Faheem. "Experimental research on wall pressure distribution in CD nozzle at mach number 1.1 for area ratio 3.24." *International Journal of Recent Technology and Engineering* 8, no. 2S3 (2019): 971-975. <https://doi.org/10.35940/ijrte.B1182.0782S319>
- [13] Rathakrishnan, E., O. V. Ramanaraju, and K. Padmanaban. "Influence of cavities on suddenly expanded flow field." *Mechanics Research Communications* 16, no. 3 (1989): 139-146. [https://doi.org/10.1016/0093-6413\(89\)90051-7](https://doi.org/10.1016/0093-6413(89)90051-7)
- [14] Viswanath, P. R., and S. R. Patil. "Zero-lift drag characteristics of afterbodies with a square base." *Journal of Spacecraft and Rockets* 34, no. 3 (1997): 290-293. <https://doi.org/10.2514/2.3231>
- [15] Viswanath, P. R. "Drag reduction of afterbodies by controlled separated flows." *AIAA Journal* 39, no. 1 (2001): 73-78. <https://doi.org/10.2514/2.1272>
- [16] Azami, Muhammed Hanafi, Mohammed Faheem, Abdul Aabid, Imran Mokashi, and Sher Afghan Khan. "Experimental research of wall pressure distribution and effect of micro jet at Mach." *International Journal of Recent Technology and Engineering* 8, no. 2S3 (2019): 1000-1003. <https://doi.org/10.35940/ijrte.B1187.0782S319>
- [17] Azami, Muhammed Hanafi, Mohammed Faheem, Abdul Aabid, Imran Mokashi, and Sher Afghan Khan. "Inspection of supersonic flows in a CD nozzle using experimental method." *International Journal of Recent Technology and Engineering* 8, no. 2S3 (2019): 996-999. <https://doi.org/10.35940/ijrte.B1186.0782S319>
- [18] Aabid, Abdul, and Sher Afghan Khan. "Determination of wall pressure flows at supersonic Mach numbers." *Materials Today: Proceedings* 38 (2021): 2347-2352. <https://doi.org/10.1016/j.matpr.2020.06.538>
- [19] Aabid, Abdul, and Sher Afghan Khan. "Studies on Flows Development in a Suddenly Expanded Circular Duct at Supersonic Mach Numbers." *International Journal of Heat and Technology* 39, no. 1 (2021): 185-194. <https://doi.org/10.18280/ijht.390120>
- [20] Zuraidi, Nur Husnina Muhamad, Sher Afghan Khan, Abdul Aabid, Muneer Baig, and Istiyaq Mudassir Shaiq. "Passive Control of Base Pressure in a Converging-Diverging Nozzle with Area Ratio 2.56 at Mach 1.8." *Fluid Dynamics & Materials Processing* 19, no. 3 (2023): 807-829. <https://doi.org/10.32604/fdmp.2023.023246>
- [21] Khan, Sher Afghan, Abdul Aabid, and Maughal Ahmed Ali Baig. "CFD analysis of CD nozzle and effect of nozzle pressure ratio on pressure and velocity for suddenly expanded flows." *International Journal of Mechanical and Production Engineering Research and Development* 8, no. 3 (2018): 1147-1158. <https://doi.org/10.24247/ijmperdjun2018119>
- [22] Aabid, Abdul, Ambareen Khan, Nurul Musfirah Mazlan, Mohd Azmi Ismail, Mohammad Nishat Akhtar, and S. A. Khan. "Numerical Simulation of Suddenly Expanded Flow at Mach 2.2." *International Journal of Engineering and Advanced Technology* 8, no. 3 (2019): 457-452.
- [23] Khan, Sher Afghan, Abdul Aabid, and C. Ahamed Saleel. "CFD simulation with analytical and theoretical validation of different flow parameters for the wedge at supersonic Mach number." *International Journal of Mechanical and Mechatronics Engineering* 19, no. 1 (2019): 170-177.
- [24] Khan, Sher Afghan, Abdul Aabid, Imran Mokashi, Abdulrahman Abdullah Al-Robaian, and Ali Sulaiman Alsagri. "Optimization of two-dimensional wedge flow field at supersonic Mach number." *CFD Letters* 11, no. 5 (2019): 80-97.
- [25] Aabid, Abdul, Azmil Afifi, Fharukh Ahmed Ghasi Mehaboob Ali, Mohammad Nishat Akhtar, and Sher Afghan Khan. "CFD analysis of splitter plate on bluff body." *CFD Letters* 11, no. 11 (2019): 25-38.
- [26] Khan, Sher Afghan, Abdul Aabid, Fharukh Ahmed Mehaboobali Ghasi, Abdulrahman Abdullah Al-Robaian, and Ali Sulaiman Alsagri. "Analysis of area ratio in a CD nozzle with suddenly expanded duct using CFD method." *CFD Letters*

- 11, no. 5 (2019): 61-71.
- [27] Khan, Sher Afghan, Abdul Aabid, and C. Ahamed Saleel. "Influence of micro jets on the flow development in the enlarged duct at supersonic Mach number." *International Journal of Mechanical and Mechatronics Engineering* 19, no. 1 (2019): 70-82.
- [28] Aabid, Abdul, Sher Afghan Khan, Maughal Ahmed Ali Baig, and K. Srinivasa Rao. "Effect of control on the duct flow at high Mach numbers." In *IOP Conference Series: Materials Science and Engineering*, vol. 1057, no. 1, p. 012053. IOP Publishing, 2021. <https://doi.org/10.1088/1757-899X/1057/1/012053>
- [29] Aabid, Abdul, Sher Afghan Khan, Maughal Ahmed Ali Baig, and Avala Raji Reddy. "Investigation of Flow Growth in a Duct Flows for Higher Area Ratio." In *IOP Conference Series: Materials Science and Engineering*, vol. 1057, no. 1, p. 012052. IOP Publishing, 2021. <https://doi.org/10.1088/1757-899X/1057/1/012052>
- [30] Al-Khalifah, Turki, Abdul Aabid, and Sher Afghan Khan. "Regression analysis of flow parameters at high mach numbers." *Solid State Technology* 63, no. 6 (2020): 5473-5488.
- [31] Afzal, Asif, Abdul Aabid, Ambareen Khan, Sher Afghan Khan, Upendra Rajak, Tikendra Nath Verma, and Rahul Kumar. "Response surface analysis, clustering, and random forest regression of pressure in suddenly expanded high-speed aerodynamic flows." *Aerospace Science and Technology* 107 (2020): 106318. <https://doi.org/10.1016/j.ast.2020.106318>
- [32] Al-Khalifah, Turki, Abdul Aabid, Sher Afghan Khan, Muhammad Hanafi Bin Azami, and Muneer Baig. "Response surface analysis of nozzle parameters at supersonic flow through microjets." *Australian Journal of Mechanical Engineering* (2021): 1-16. <https://doi.org/10.1080/14484846.2021.1938954>
- [33] Aabid, Abdul, and Sher Afghan Khan. "Investigation of high-speed flow control from CD nozzle using design of experiments and CFD methods." *Arabian Journal for Science and Engineering* 46, no. 3 (2021): 2201-2230. <https://doi.org/10.1007/s13369-020-05042-z>
- [34] Khan, Umair, William Pao, Nabihah Sallih, and Farruk Hassan. "Flow Regime Identification in Gas-Liquid Two-Phase Flow in Horizontal Pipe by Deep Learning." *Journal of Advanced Research in Applied Sciences and Engineering Technology* 27, no. 1 (2022): 86-91. <https://doi.org/10.37934/araset.27.1.8691>
- [35] Abidin, Nurul Hafizah Zainal, Nor Fadzillah Mohd Mokhtar, Izzati Khalidah Khalid, and Siti Nur Aisyah Azeman. "Oscillatory Mode of Darcy-Rayleigh Convection in a Viscoelastic Double Diffusive Binary Fluid Layer Saturated Anisotropic Porous Layer." *Journal of Advanced Research in Numerical Heat Transfer* 10, no. 1 (2022): 8-19.
- [36] Rusdi, Nadia Diana Mohd, Siti Suzilliana Putri Mohamed Isa, Norihan Md Arifin, and Norfifah Bachok. "Thermal Radiation in Nanofluid Penetrable Flow Bounded with Partial Slip Condition." *CFD Letters* 13, no. 8 (2021): 32-44. <https://doi.org/10.37934/cfdl.13.8.3244>
- [37] Aabid, Abdul, S. Afghan Khan, and Muneer Baig. "Numerical analysis of a microjet-based method for active flow control in convergent-divergent nozzles with a sudden expansion duct." *Fluid Dynamics & Materials Processing* (2022): 1-24. <https://doi.org/10.32604/fdmp.2022.021860>
- [38] Tu, Jiyuan, Guan Heng Yeoh, and Chaoqun Liu. *Computational fluid dynamics: a practical approach*. Butterworth-Heinemann, 2018.
- [39] Pandey, K. M., and E. Rathakrishnan. "Annular cavities for Base flow control." *International Journal of Turbo and Jet Engines* 23, no. 2 (2006): 113-128. <https://doi.org/10.1515/TJJ.2006.23.2.113>
- [40] Oosthuizen, Patrick H., and William E. Carscallen. *Introduction to compressible fluid flow*. 2nd ed. CRC Press, 2014. <https://doi.org/10.1201/b15414>